

See discussions, stats, and author profiles for this publication at: <https://www.researchgate.net/publication/261741463>

Gly25–Ser26 Amyloid β -Protein Structural Isomorphs Produce Distinct A β 42 Conformational Dynamics and Assembly Characteristics

ARTICLE *in* JOURNAL OF MOLECULAR BIOLOGY · APRIL 2014

Impact Factor: 4.33 · DOI: 10.1016/j.jmb.2014.04.004 · Source: PubMed

CITATIONS

8

READS

70

8 AUTHORS, INCLUDING:



[Robin Roychaudhuri](#)

Johns Hopkins Medicine

19 PUBLICATIONS 451 CITATIONS

[SEE PROFILE](#)



[Xueyun Zheng](#)

University of California, Santa Barbara

11 PUBLICATIONS 79 CITATIONS

[SEE PROFILE](#)

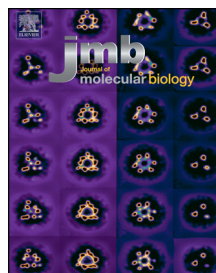


[David Teplow](#)

University of California, Los Angeles

244 PUBLICATIONS 26,269 CITATIONS

[SEE PROFILE](#)



Gly25-Ser26 Amyloid β -Protein Structural Isomorphs Produce Distinct A β 42 Conformational Dynamics and Assembly Characteristics

Robin Roychaudhuri¹, Aleksey Lomakin², Summer Bernstein³,
Xueyun Zheng³, Margaret M. Condron¹, George B. Benedek²,
Michael Bowers³ and David B. Teplow^{1,4}

1 - Department of Neurology, David Geffen School of Medicine at University of California Los Angeles, Los Angeles, CA 90095, USA

2 - Department of Physics and Center for Materials Science and Engineering, Massachusetts Institute of Technology, Cambridge, MA 02139, USA

3 - Department of Chemistry and Biochemistry, University of California Santa Barbara, Santa Barbara, CA 93106, USA

4 - Molecular Biology Institute and Brain Research Institute, University of California Los Angeles, Los Angeles, CA 90095, USA

Correspondence to David B. Teplow: Department of Neurology, David Geffen School of Medicine at University of California Los Angeles, 635 Charles E. Young Drive South (Room 445), Los Angeles, CA 90095, USA. dteplow@ucla.edu
<http://dx.doi.org/10.1016/j.jmb.2014.04.004>

Edited by J. Clarke

Abstract

One of the earliest events in amyloid β -protein (A β) self-association is nucleation of A β monomer folding through formation of a turn at Gly25-Lys28. We report here the effects of structural changes at the center of the turn, Gly25-Ser26, on A β 42 conformational dynamics and assembly. We used “click peptide” chemistry to quasi-synchronously create A β 42 from 26-O-acetyliso-A β 42 (iA β 42) through a pH jump from 3 to 7.4. We also synthesized N α -acetyl-Ser26-iA β 42 (Ac-iA β 42), which cannot undergo O \rightarrow N acyl chemistry, to study the behavior of this ester form of A β 42 itself at neutral pH. Data from experiments monitoring increases in β -sheet formation (thioflavin T, CD), hydrodynamic radius (R_h), scattering intensity (quasielastic light scattering spectroscopy), and extent of oligomerization (ion mobility spectroscopy–mass spectrometry) were quite consistent. A rank order of Ac-iA β 42 > iA β 42 > A β 42 was observed. Photochemically cross-linked iA β 42 displayed an oligomer distribution with a prominent dimer band that was not present with A β 42. These dimers also were observed selectively in iA β 42 in ion mobility spectrometry experiments. The distinct biophysical behaviors of iA β 42 and A β 42 appear to be due to the conversion of iA β 42 into “pure” A β 42 monomer, a nascent form of A β 42 that does not comprise the variety of oligomeric and aggregated states present in pre-existent A β 42. These results emphasize the importance of the Gly25-Ser26 dipeptide in organizing A β 42 monomer structure and thus suggest that drugs altering the interactions of this dipeptide with neighboring side-chain atoms or with the peptide backbone could be useful in therapeutic strategies targeting formation of A β oligomers and higher-order assemblies.

© 2014 Elsevier Ltd. All rights reserved.

Introduction

Alzheimer's disease (AD) is a fatal neurodegenerative disorder linked particularly strongly to the pathologic assembly of a 42-residue form of the amyloid β -protein (A β), A β 42 [1,2]. Pathognomonic features of AD include extracellular amyloid plaques containing fibrillar A β and intracellular neurofibrillary tangles containing tau protein [3]. A prominent working hypothesis of AD pathogenesis focuses on

the role(s) of oligomeric A β assemblies [4]. If a particular A β isoform is the proximate neurotoxin in AD, then knowledge-based design of therapeutic agents requires elucidation of the structural biology of A β monomer folding and oligomerization.

Biochemical, nuclear magnetic resonance spectroscopy, and computational studies of A β monomer dynamics have revealed a 10-residue segment, $^{21}\text{Ala-Glu-Asp-Val-Gly-Ser-Asn-Lys-Gly-Ala}^{30}$, that forms a turn-like structure nucleating A β monomer

folding [5–10]. Structural changes in this region caused by familial AD-linked or cerebral amyloid angiopathy-linked amyloid β -protein precursor mutations have been shown to destabilize this turn nucleus, facilitating A β assembly [6,9,11]. Computational studies have revealed that hydrogen bond formation can occur between the oxygen atoms of the Asp23 carboxylate anion and the amide hydrogens of Gly25, Ser26, Asn27, and Lys28. The Asp23-Ser26 hydrogen bond had the highest occurrence frequency [8], suggesting that the interaction of these two amino acids could be

particularly important in organizing A β structure. In addition, Ser26 formed a 3_{10} helix with Asn27 and Lys28 [8]. Interestingly, Ser26 also appears to be important in controlling the structure of the APP juxtamembrane region ($^{25}\text{Gly}-\text{Ser}-\text{Asn}-\text{Lys}^{28}$). This turn region, which includes Lys28, mediates interaction with the γ -secretase complex and affects the peptide bond specificity of the complex, resulting in alterations in the distribution of A β peptide lengths produced [12–15]. The structural dynamics involving Ser26 thus have relevance not only for understanding A β assembly but also for understanding *de novo*

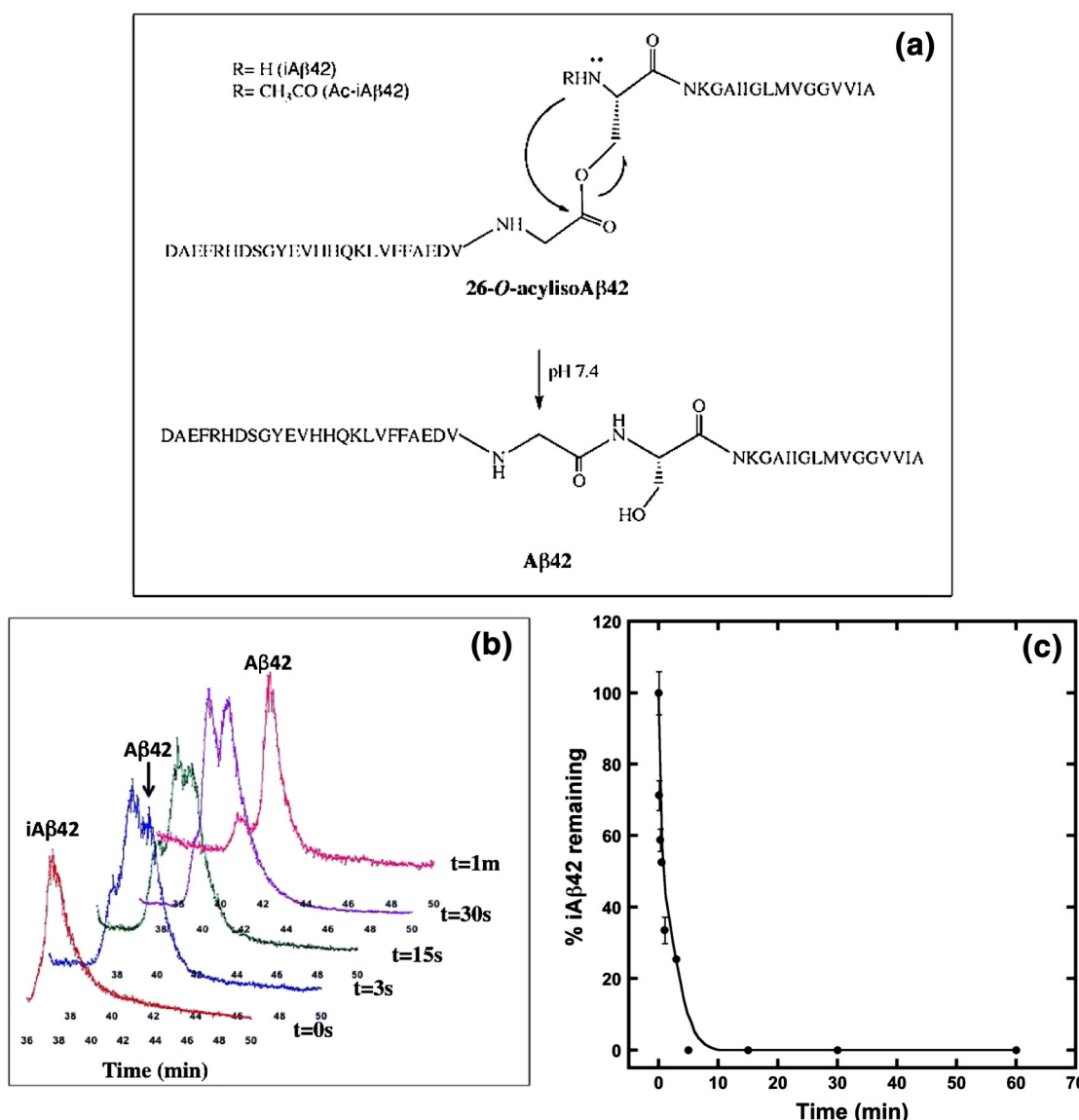


Fig. 1. “Click peptide” chemistry. (a) *i*A β 42-to-A β 42 conversion scheme. (b) Conversion of *i*A β 42 to A β 42. The figure shows conversion of *i*A β 42 to A β 42 upon incubation at pH 7.5 monitored on a RP-HPLC C₁₈ column. (c) Kinetics of conversion of *i*A β 42 to A β 42 at pH 7.5. Half-time ($t_{1/2}$) of the conversion reaction in *i*A β 42 was determined using RP-HPLC followed by area under the peak quantitation at the different time intervals using Peak Simple chromatographic analysis software.

A β production. For these reasons, we sought to elucidate more fully the role of Ser26 in this dynamics.

Fortunately, concurrent with our studies of A β structural dynamics, an improved method for the solid-phase peptide synthesis of A β 42, which presents a number of synthetic and preparative challenges, was developed. This method involved the synthesis of an A β 42 isomer as a “click peptide” [16]. This strategy, originally developed by Sohma *et al.* [17,18], involves synthesis of 26-O-acyliso-A β 42 (iA β 42), which is identical in primary structure with normal human A β , except that Gly25 and Ser26 are linked through an ester bond (Fig. 1a). This ester form of A β 42 displays significantly decreased on-resin β -sheet formation, which increases synthetic efficiency, and produces a crude product that is \approx 100-fold more soluble than A β 42, which increases yields during peptide purification. In the formation of A β 42 from iA β 42, all that is required is a pH shift from a strongly acidic regime to a neutral or basic one. In the basic pH regime, iA β 42 rapidly ($t_{1/2} \approx 30$ s) isomerizes into A β 42, yielding the native Gly25-Ser26 peptide bond [17,19].

The substantial differences in chemical synthesis and purification behavior of iA β 42 relative to A β 42 suggested that this peptide would be especially useful for evaluating the role of the Gly25-Ser26 dipeptide region in controlling A β assembly. Importantly, such studies are facilitated by the ability to produce native A β 42 peptide quasi-synchronously from iA β 42 through a simple increase in pH. This latter ability would mitigate problems with pre-assay aggregation of A β 42, problems that have complicated the interpretation of much experimental data [20]. We report and discuss here the results of such studies.

Results

Kinetics of O \rightarrow N acyl migration

The *in vitro* study of A β assembly is complicated by technical problems related to peptide preparation and use (for a review, see Ref. [21]). These problems are especially relevant to studies of A β 42, which is thought to be the key A β isoform linked to AD pathogenesis [4]. To circumvent this problem, we utilized a novel “click peptide” chemistry [17,19] to produce A β 42 quasi-synchronously *in situ* through pH-induced O \rightarrow N acyl migration within iA β 42 (Fig. 1a).

To determine the half-time ($t_{1/2}$) for conversion of iA β 42 to A β 42, we dissolved lyophilized iA β 42 at pH 8.0 and monitored A β 42 production by reverse-phase high-performance liquid chromatography (RP-HPLC). An \approx 1.5-min shift in peak position is

indicative of conversion (Fig. 1b). Analysis of the conversion kinetics revealed $t_{1/2} \approx 30$ s (Fig. 1c). A β 42 monomer production from iA β 42 thus may be considered quasi-synchronous relative to the much longer half-times for the evolution of ordered secondary structure, β -sheet formation, protofibril formation, and fibril formation ($t_{1/2} \approx 2$ –13 days) [21,22]. Quasi-synchronous production of A β 42 *in situ* should decrease interpretive complications caused by the structural heterogeneity that usually exists in starting A β 42 populations [21].

We also synthesized N α -acetyl-Ser26-iA β 42 (Ac-iA β 42) because the O \rightarrow N acyl shift necessary to produce A β 42 does not occur in this peptide. As predicted, the amount of Ac-iA β 42 observed during the 60-min incubation at pH 7.5 remained constant (data not shown). The Ac-iA β 42 peptide was used throughout our experiments as a “non-clickable” control, that is, a peptide in which an O \rightarrow N acyl shift could not occur and thus one that remained in an ester form. Importantly, this peptide also allowed us to study how an acetyl group, instead of a hydrogen atom, on the N α atom of Ser26 affected the peptide's conformational and assembly properties.

Time evolution of ThT fluorescence

To begin comparative analysis of A β 42, iA β 42, and Ac-iA β 42 assembly, we sought first to monitor the temporal development of β -sheet-rich fibrils. To do so, we used the technique of thioflavin T (ThT)

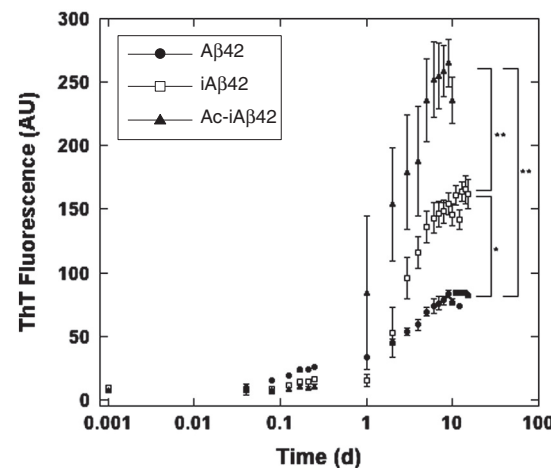


Fig. 2. Kinetics of ThT fluorescence development. iA β 42, Ac-iA β 42, and A β 42. We incubated 20 μ M of the individual peptides with 40 μ M ThT at pH 7.5 and 37 °C with shaking and read them in a 96-well microtiter plate reader at excitation wavelength of 450 nm and emission wavelength of 482 nm. Figure shows logarithmic plot of ThT fluorescence (arbitrary units) *versus* time (days). Error bars refer to SD. Statistical analyses were performed using SigmaStat statistical analysis software. (*) and (**) are $p = 0.002$ and $p < 0.001$, relative to A β 42).

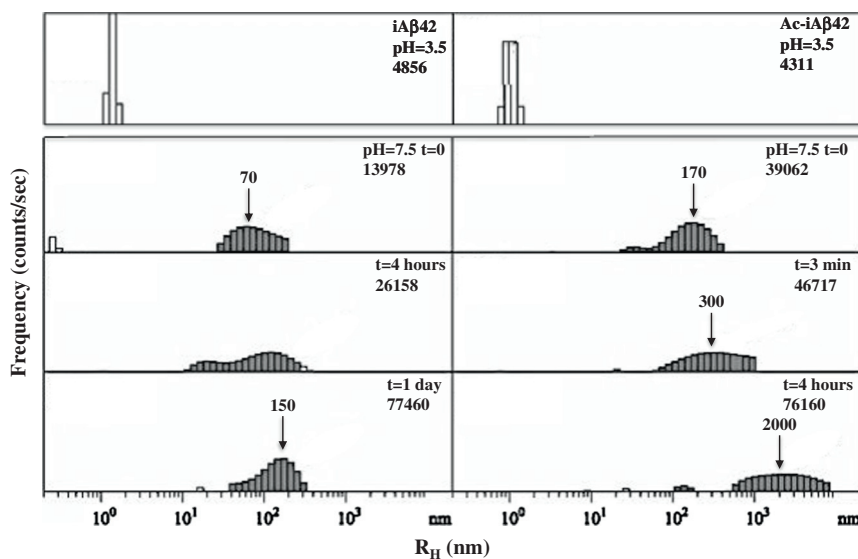


Fig. 3. QLS spectroscopy. QLS was used to monitor the kinetics of assembly of iA β 42 (left) and Ac-iA β 42 (right) at pH 3.5 (top panel) and 7.5 (lower panels). Plot of intensity (counts/s) versus hydrodynamic radius (R_H in nanometer). Arrows indicate increasing particle size over time.

fluorescence, which in the A β system has been shown to correlate highly with β -sheet formation [23–25]. As shown in Fig. 2, lag phases for A β 42, iA β 42, and Ac-iA β 42 were \approx 1 h, \approx 1 day, and \approx 8 h. Ac-iA β 42 then showed a rapid increase in ThT fluorescence that plateaued at \leq 10 days. iA β 42 had a slower rate of assembly and a fluorescence plateau at \approx 10 days. A β 42 displayed the slowest rate of ThT fluorescence increase and a plateau also at \approx 10 days. The relative rates of increase in ThT fluorescence thus were Ac-iA β 42 > iA β 42 > A β 42 (Fig. 2).

Monitoring oligomerization using quasielastic light scattering spectroscopy

We used quasielastic light scattering spectroscopy (QLS) as an orthogonal method to non-invasively monitor A β assembly (for a review of QLS applied to the A β system, see Refs. [26–28]). We first monitored samples of iA β 42 and Ac-iA β 42 in 0.2 mM sodium acetate, pH 3.5, at concentrations of approximately 77 μ M and 154 μ M, respectively. Only background scattering was detected throughout the initial observation period (see Figs. S1a and b). Such low scattering intensity at these concentrations indicates that the peptide is predominately in a monomeric state. A pH jump to 7.5 then was executed at 74 h for iA β 42 and 75.2 h for Ac-iA β 42 [Fig. 3 and Fig. S1a (arrow) and S1b (arrow)]. The iA β 42 samples immediately showed substantial scattering from particles with a wide distribution of sizes centered at \approx 70 nm. The particles continued to increase in size, with the average size of the

particles roughly doubling every day of incubation (Fig. S1a). Ac-iA β 42 showed immediate, even greater, aggregation. The initial aggregation rate was so high that no transition from low intensity to higher intensity was observed (Fig. S1b), as had been seen with iA β 42 (Fig. S1a). Indeed, in the first 3 min of measurement, the particle distribution was centered at $R_H \approx$ 170 nm, whereas in the second 3 min, the distribution maximum was centered at $R_H \approx$ 300 nm. After 4 h, particles of \approx 2000 nm were observed (Fig. 3, right panel).

We then conducted a series of experiments in which A β samples were dissolved directly in 20 mM sodium phosphate, pH 7.5, at concentrations of 0.5 mg/ml, and then filtered using a 20-nm pore size Anotop filter. These samples initially produced only background scattering (Fig. 4, left panels), but scattering from particles was observed after several hours. The lag times[†], during which no scattering from the peptides was observed, are listed in Table 1. Following this time, aggregation was observed and the rates of aggregation, dR_H/dt , for the different peptides were found to vary substantially (Table 1 and Fig. S2). A β 42 assemblies increased in size at the rate of 2 nm/h, whereas iA β 42 and Ac-iA β 42 aggregates increased in size 4–5 times faster (8.5 and 10.0 nm/h, respectively; Fig. S2). The intensity of scattering from aggregates of all three samples remained small compared to the background scattering for several more hours, but eventually increased abruptly, displaying a third-order dependence on particle size (Fig. 4). Because iA β 42 and Ac-iA β 42 aggregated much faster than did A β 42, the lag time (Table 1) for A β 42

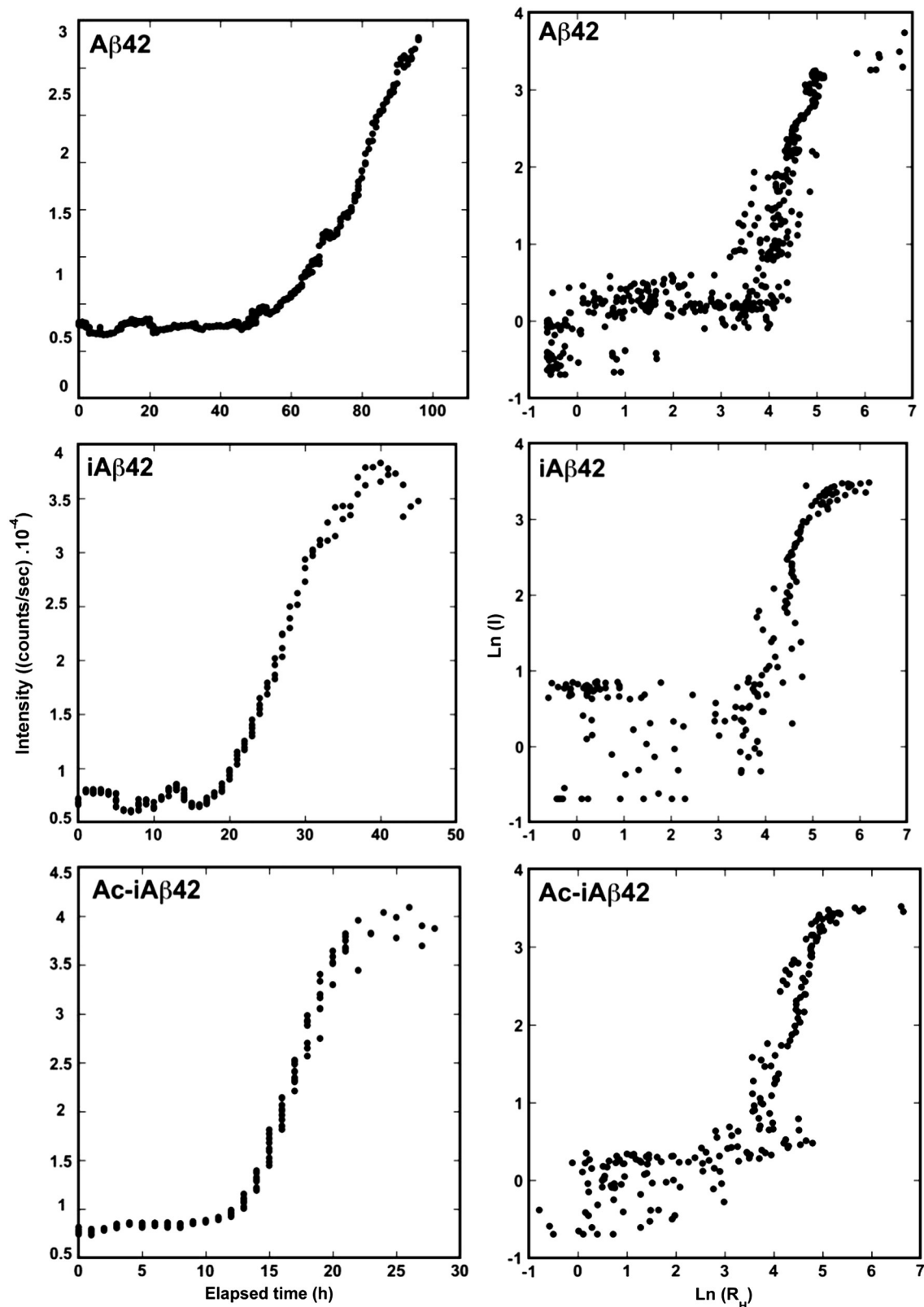


Fig. 4. Kinetics of scattering intensity increases. QLS was used to monitor the pH-induced conversion of $A\beta 42$, $iA\beta 42$, and $Ac-iA\beta 42$. Left column: Plots of intensity (counts/s) *versus* elapsed time (h). Right column: Plots of \ln of intensity [$\ln(I)$] *versus* \ln of hydrodynamic radius [$\ln(R_h)$]. Note that the time scales for each peptide differ from 100 h ($A\beta 42$) to 50 h ($iA\beta 42$) to 30 h ($Ac-iA\beta 42$).

is significantly longer than for iA β 42 and Ac-iA β 42. These data are consistent with the previously determined rank order of β -sheet formation rates determined by ThT fluorescence, namely Ac-iA β 42 > iA β 42 > A β 42.

Probing protein conformation using limited proteolysis

We next sought to probe the initial conformational states of the three peptides to determine if any relationship existed between these states and the assembly process, as determined by ThT and QLS. To do so, we performed limited proteolysis experiments using porcine pepsin and proteinase K. Limited proteolysis experiments previously revealed a structurally stable A β folding nucleus [10] and were used to compare turn stabilities ($\Delta\Delta G_f$) among A β peptides containing cerebral amyloid angiopathy-linked or AD-linked amino acid substitutions [6].

Here, we began our experiments at pH 2.0, a condition under which iA β 42 conversion cannot occur. We used the endoproteinase pepsin, a relatively non-specific protease with maximal activity at pH 2.0 that cleaves at hydrophobic and aromatic residues in the P1' position [29] (Phe, Val, Ala, Ile, Tyr, Trp, and Leu) if a hydrophobic residue is present at the P1 position. Time-dependent increases in proteolysis were readily apparent in the RP-HPLC chromatograms with A β 42 displaying levels of cleavage of \approx 15% at 15 min and \approx 55% at 90 min (Fig. 5a). In contrast, \approx 70% cleavage of iA β 42 was observed at 15 min and \approx 80% cleavage was observed at 90 min. Ac-iA β 42 was cleaved similarly to A β 42 (\approx 30% at 15 min and \approx 50% at 90 min). The differences in cleavage levels among the peptides at 15 min were highly significant. The data suggest that pepsin-sensitive peptide bonds within iA β 42 are more accessible initially than are those same bonds in A β 42 or Ac-iA β 42.

To determine if differences in protease sensitivity existed among A β 42, A β 42 formed by conversion of iA β 42, and Ac-iA β 42, we repeated the protease digestion experiments at pH 7.5. Pepsin is inactive

at pH 7.5; thus, we used proteinase K because of its pH optimum (pH 8) and wide substrate specificity, which increases the sensitivity of the system to

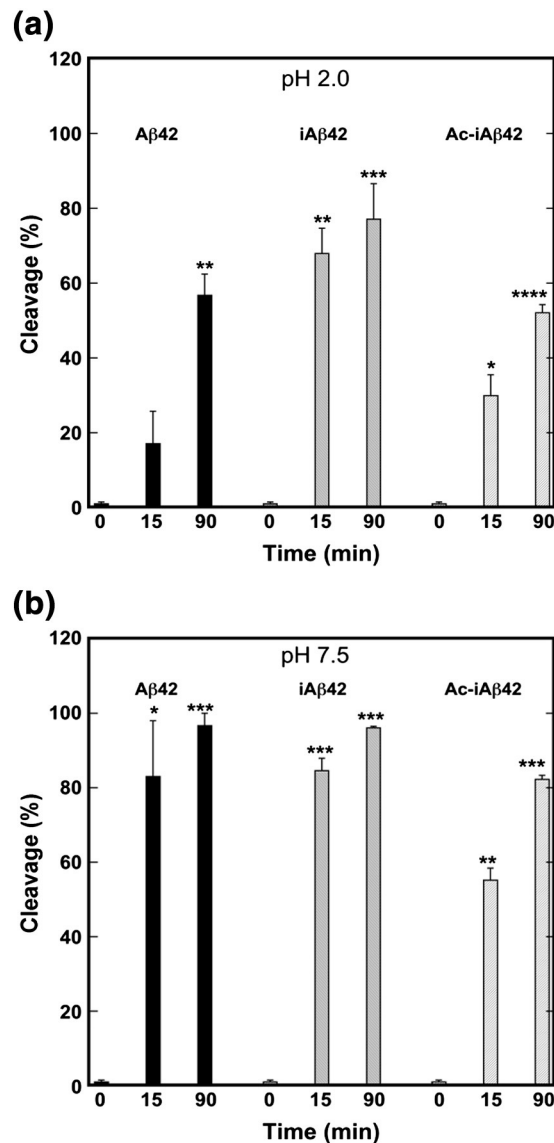


Fig. 5. Probing peptide structure using limited proteolysis. A β 42, iA β 42, and Ac-iA β 42 were subjected to limited proteolysis with pepsin at pH 2.0 (a) or with proteinase K at pH 7.5 (b). Aliquots of the reaction mixture were removed at 0, 15, and 90 min and then analyzed by RP-HPLC. The area of the peak representing uncleaved A β was estimated using the peak integration feature in Peak Simple chromatographic data analysis software. This area was used to calculate cleavage percent according to the formula $C_t = (A_0 - A_t) \times 100/A_0$, where C_t is cleavage percent, A_0 is initial area of A β HPLC peak, and A_t is area of A β peak at time t . Statistical analyses, performed using SigmaStat statistical analysis software, determined the significance of differences between samples at $t = 0$ and subsequent time points. (a) * $p = 0.03$, ** $p = 0.01$, *** $p < 0.02$, and **** $p = 0.002$; (b) * $p = 0.03$, ** $p = 0.02$, and *** $p < 0.001$.

Table 1. QLS spectroscopy

Sample	Lag time (h)	dR_H/dt (nm/h)
A β 42	24.5	2.0
iA β 42	10.5	8.5
Ac-iA β 42	6.5	10.0

Kinetic parameters of iA β 42, Ac-iA β 42, and native A β 42 during quasi-synchronous assembly. Lag time is defined as the period between initial sample preparation/monitoring and the beginning of continuous increases in R_H . This time is determined by establishing the point of intersection of two lines, one fitted to the initial quasi-constant portion of the progress curve and the other fitted to that portion in which persistent increases in R_H are observed. This latter curve fit also is used to establish dR_H/dt , the change in hydrodynamic radius per unit time.

conformational differences. A β 42 and iA β 42 were cleaved similarly, with 80–90% cleavage observed at 15 min and almost complete cleavage seen at 90 min (Fig. 5b). Ac-iA β 42 was more resistant to cleavage, displaying 60% cleavage at 15 min and ~80% cleavage at 90 min.

Conformational dynamics determined by CD spectroscopy

We used CD spectroscopy to monitor temporal changes in peptide backbone conformation (Fig. 6a–c). The spectra for A β 42, iA β 42, and Ac-iA β 42 at pH 7.5 show clear differences in assembly kinetics. A β 42 exists as a statistical coil at $t = 0$ h. A transition to a mixed α/β conformer occurs between 60 and 180 min, before a predominately β -sheet population is observed at ≈ 6 h (Fig. 6a). iA β 42 showed a much

slower transition to β -sheet (Fig. 6b), displaying substantial statistical coil for ≈ 9 h, at which time a transition to β -sheet was observed. The mixed α/β conformation seen in A β 42 was not prominent in this experiment, although some mixed conformation was observed at 19 h. Ac-iA β 42, in contrast to both A β 42 and iA β 42, displayed a mixed α/β conformation at the initial time point ($t = 0$ h) and converted rapidly (90 min) to β -sheet (Fig. 6c). The rapid conformational conversion of Ac-iA β 42 to β -sheet is consistent with its high aggregation propensity. The fact that A β 42 converts faster than does iA β 42 (Fig. 6d) is consistent with the interpretation of the low pH limited proteolysis results, namely that A β 42 initially is more folded or aggregated than is the newly formed iA β 42. (Parenthetically, these data demonstrate in a practical manner the theoretical value of the click peptide strategy for producing A β 42.)

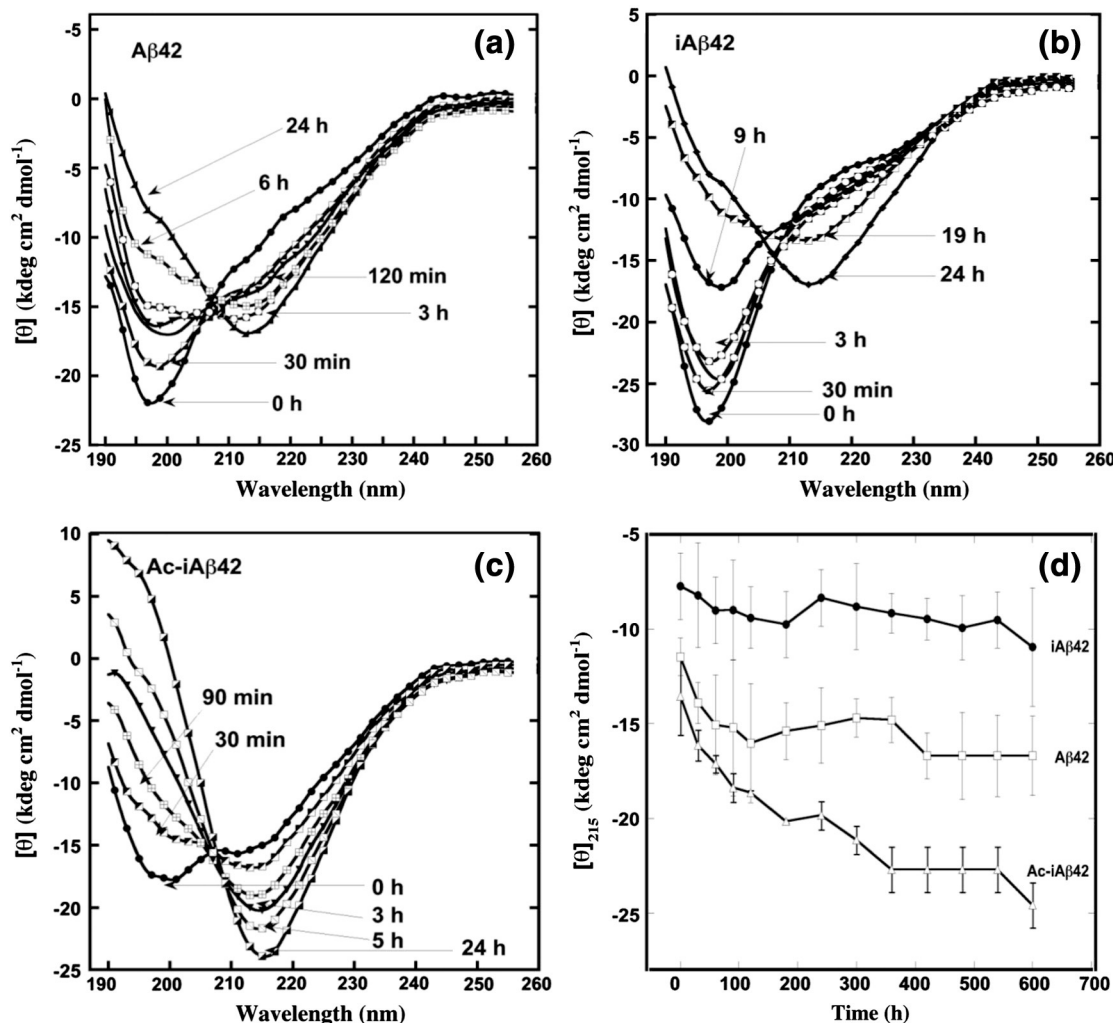


Fig. 6. CD spectroscopy. Secondary structure dynamics was characterized using CD during incubation of peptides at pH 7.5, 37 °C, with gentle shaking. Peptides were (a) A β 42, (b) iA β 42, and (c) Ac-iA β 42. (d) β -Sheet ellipticities of A β 42, iA β 42, and Ac-iA β 42 at 215 nm versus time.

Determination of the A β oligomer size distribution by ion mobility spectroscopy–mass spectrometry

Mass spectra and arrival time distributions (ATDs) for A β 42, iA β 42, and Ac-iA β 42 are shown in Fig. S3 and Fig. 7, respectively. A β 42 has been characterized previously by ion mobility spectroscopy–mass spectrometry (IMS–MS) [14,30] and some of these data were included here for the purpose of direct comparison. The negative ion spectra of iA β 42, 20 min and 2 h after dissolution at pH 7.4, are shown in Fig. S3a and b, respectively. At 20 min, only the -3 and -4 monomer charge states are present. After 2 h of incubation, a new peak appears at $z/n = -5/2$ that must be due to oligomers [14] and indicates that early aggregation states of A β 42 are being observed in real time. The mass spectrum of Ac-iA β 42 is shown in Fig. S3c. Unlike the A β 42 and iA β 42 spectra, that of Ac-iA β 42 is dominated by a broad collection of unresolved peaks, indicative of rapid aggregation. The ammonium acetate concentration had to be reduced to 0.1 mM to observe a resolved mass spectrum. This drop in buffer concentration dramatically reduced the rate of aggregation and yielded the spectrum shown in Fig. S3d, which is similar to that of iA β 42 (Fig. S3b).

ATDs for iA β 42 were obtained for each charge state in the 2-h mass spectrum of Fig. S3b and compared with ATDs of A β 42 (Fig. 7a and b). The ATDs for the $z/n = -3$ ions of A β 42 and iA β 42 are shown in Fig. 7a. In previous studies of A β 42, the -3 charge state ATD revealed two distinct features that were unambiguously assigned to two different monomeric structures (M1 and M2) [30,31]. The analysis of these results showed that M1 is a gas-phase structure dominated by exposed hydrophobic residues and M2 is a dehydrated solution-like structure [8].

The two dominant features observed in the ATDs of iA β 42, labeled M1 and M2 in Fig. 7a, are clearly similar to those previously reported for A β 42. What is unique is the small feature at 450 μ s observed in the 100 eV ATD of iA β 42 (Fig. 7a). This feature became more intense at lower injection energy (30 eV) and thus most likely is the -6 dimer (labeled D). This peak is not observed in the A β 42 ATD; thus, it may be due to the dimerization of iA β 42 prior to isomerization or to the formation of the iA β 42:A β 42 heterodimer concurrent with iA β 42 conversion to A β 42. The cross-section for this dimer is much larger than the $z/n = -5/2$ dimer (Table 2) and is consistent with it having a significantly different structure.

The ATDs for the $z/n = -5/2$ ions of iA β 42 were acquired at three different injection energies, ranging from 30 to 100 eV, and are compared directly with the ATDs of A β 42 in Fig. 7b. A detailed discussion of injection energy methods and assignment of the features is given in Bernstein *et al.* [30]. With the use of the same analytical methods, the following

oligomerization states are assigned to the features shown in the ATD of Fig. 7b: D, dimer; Te, tetramer; H, hexamer; and (H)₂, dodecamer (likely formed from stacking two planar hexamers) [14]. A shoulder to the right of the (H)₂ peak most likely corresponds to the decamer (P)₂, where P is pentamer. No octamer was observed. The features observed for iA β 42 were assigned by analogy to A β 42 (Fig. 7b).

The ATDs for A β 42 and iA β 42 are very similar at high and medium injection voltages. However, at low injection voltages, where solution oligomer distributions are most closely retained, they are quite different. Both have a significant dodecamer peak, but A β 42 has a strong hexamer peak, while iA β 42 has essentially no hexamer peak and strong tetramer and dimer peaks. These differences must reflect differences in assembly. The dimer and tetramer peaks in the iA β 42 ATD likely are due to A β 42:iA β 42 heterooligomers (as discussed above) and these mixed oligomers do not further aggregate.

The ATDs allow collision cross-sections (σ) to be determined. The ATD for the Ac-iA β 42 $z/n = -5/2$ charge state initially was broad and comprised three distinct features (data not shown). After several hours of incubation, new features appeared. Assignments of these features were made by direct comparison to the ATDs of A β 42 and iA β 42 (Fig. S4a and b). The ATDs are plotted here as a function of σ/n to normalize the experimental differences of pressure and temperature between experiments. As in A β 42 and iA β 42, features corresponding to H₂, P₂, H, Te, and some D appear to be present in Ac-iA β 42 (Fig. S4c), although resolution of the D, Te, and H species is not clearly obtained. The σ/n values and the absolute cross-sections are listed in Table 2 for A β 42, iA β 42, and Ac-iA β 42.

Determination of the A β oligomer size distribution by PICUP

To monitor oligomer size distributions *in hydro*, we used photo-induced cross-linking of unmodified proteins (PICUP) followed by SDS-PAGE and silver staining (Fig. 8a). The three study peptides were cross-linked immediately after dissolution and filtration ($t = 0$ h) and also after incubation at RT (room temperature) for 26 h without shaking (to monitor changes in oligomerization detectable with PICUP chemistry). At $t = 0$ h and pH 7.5, A β 42 displayed an intense monomer band, weak dimer and trimer bands, and intense bands corresponding to tetramer, pentamer, and hexamer. A faint heptamer band also was observed. The distribution at 26 h was identical, within experimental error. iA β 42 displayed a similar distribution to A β 42 at $t = 0$ h, except that an intense dimer band also was observed. The iA β 42 distribution at $t = 26$ h was similar to that at $t = 0$ h. The oligomer distribution of Ac-iA β 42 was distinct from those of A β 42 or iA β 42. This distribution

included a very faint monomer band, an intense dimer band, an additional band at a position just above dimer (2+), and a faint band visible slightly above the position of trimer in the case of the $t = 0$ h time point. The distributions of Ac-iA β 42 also changed little between 0 and 26 h. Quantification and normalization of band intensities was performed to allow quantitative comparisons among the oligomer distributions (Table 3).

iA β 42 does not convert to A β 42 at pH 3.0. Although this pH is not physiologic, we were curious whether the different primary structures would produce different oligomerization patterns in this system. We found that the distribution of A β 42 at $t = 0$ h at pH 3.0 differed considerably from that seen at pH 7.5. The pH 3.0 distribution displayed an intense monomer band along with a series of bands appearing to range from dimer to heptamer, each of which had an intensity that was inversely proportional to its order (Table 4). A smaller band

below the monomer (*) in Fig. 8b) is seen, suggesting the presence of two closely related conformers. This type of distribution is characteristic of systems in which simple diffusion-limited cross-linking occurs, as opposed to the system at pH 7.5 in which preformed oligomers exist [32]. No difference in the distribution pattern was seen at 26 h. iA β 42, in contrast, displayed a faint band migrating at a position between that of monomer and dimer and a more intense band at a position slightly above dimer. It was not possible to determine if a trimer band existed or whether the dimer electrophoresed as an intense band with some protein trailing behind. The iA β 42 distributions at 0 and 26 h were similar. Ac-iA β 42, in contrast to both A β 42 and iA β 42, produced a distribution at 0 h with a relatively weak doublet monomer band, followed by intense dimer, trimer, and tetramer bands. A light pentamer band also was observed (Fig. 8b). This distribution was identical, within experimental error, at 26 h.

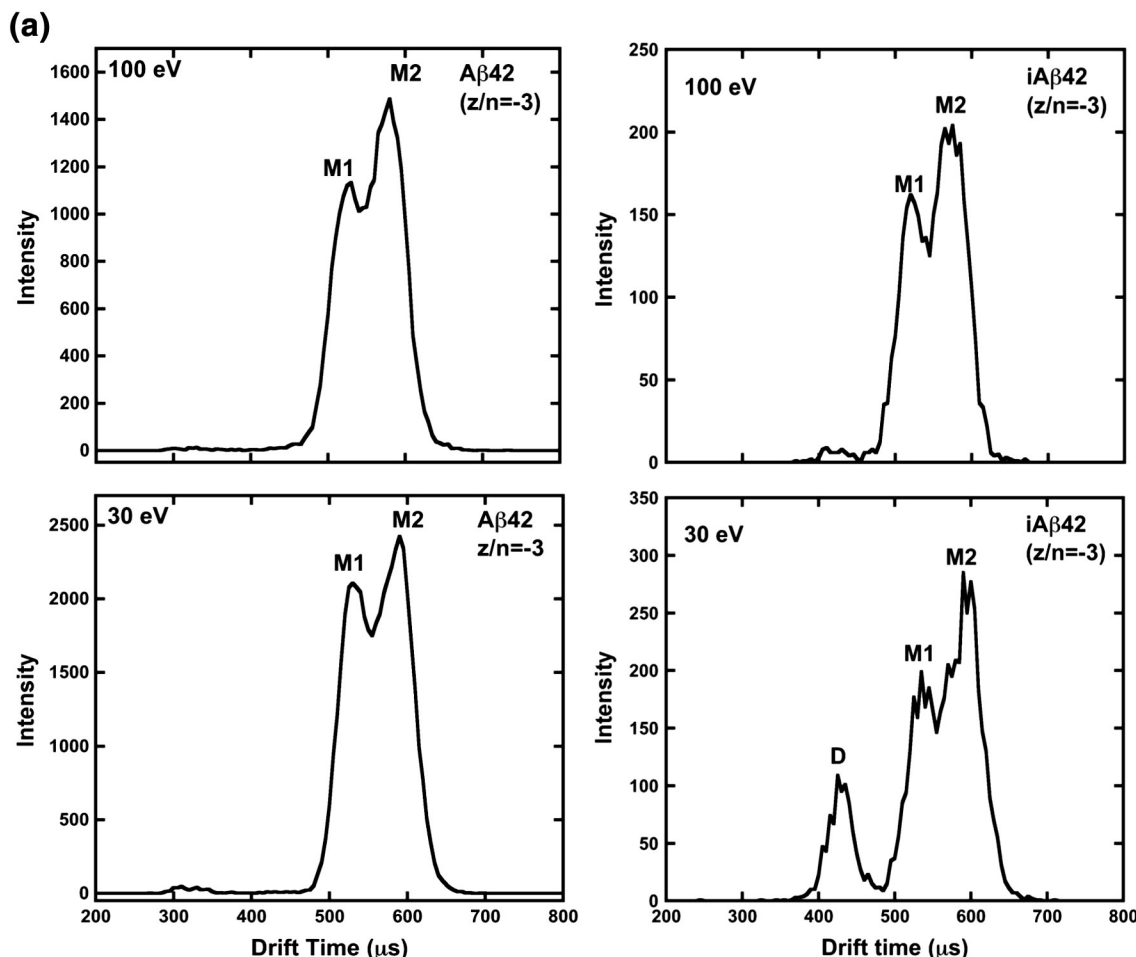


Fig. 7. Ion mobility spectrometry–mass spectrometry. (a) ATDs of the $z/n = -3$ charge state of A β 42 and iA β 42 at 100 eV and 30 eV. (b) ATDs of the $z/n = -5/2$ charge state of A β 42 and iA β 42 → A β 42 and at 100, 50, and 30 eV injection voltages.

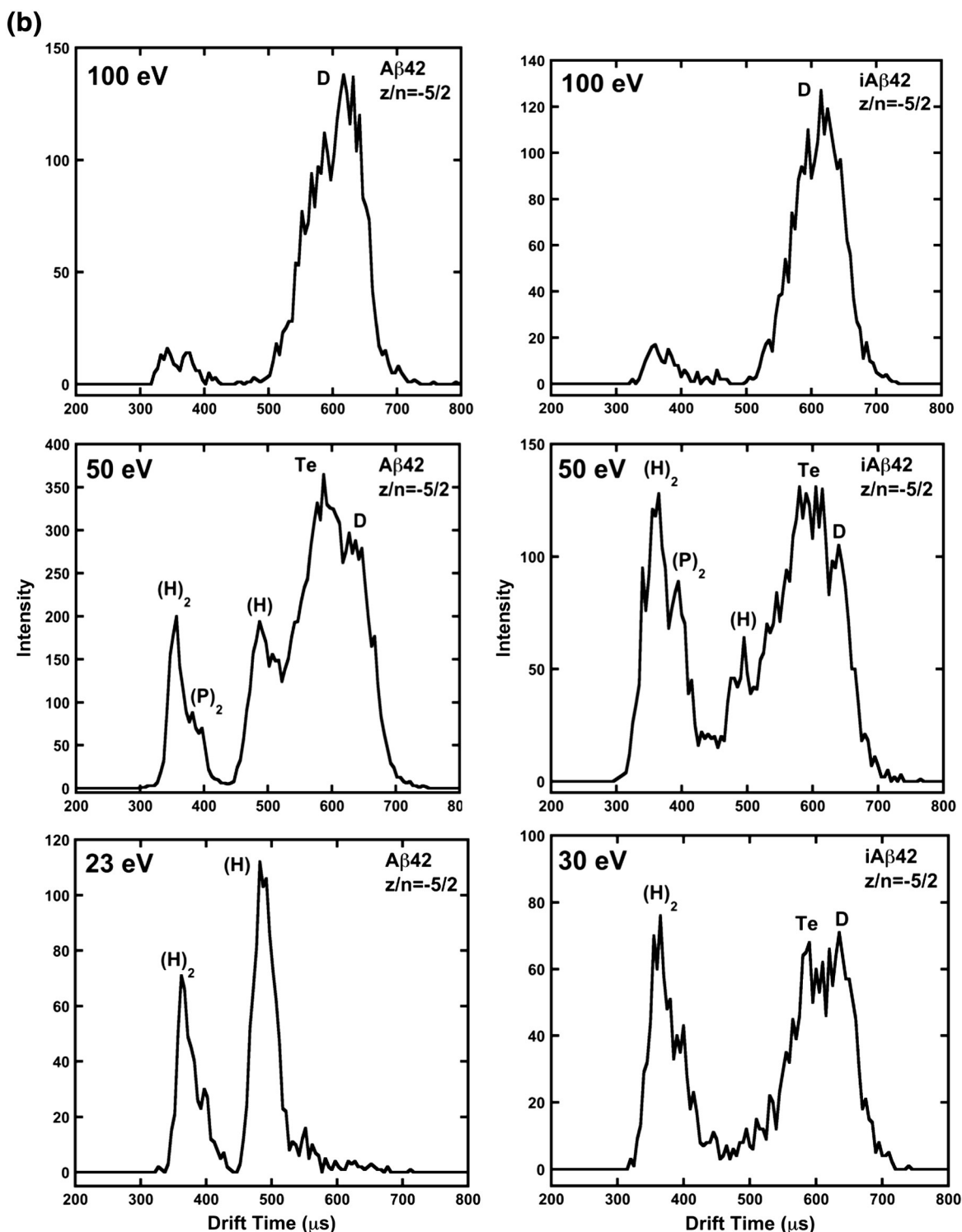


Fig. 7. (continued).

Assembly morphology

To determine the morphologies of the peptide assemblies, we performed electron microscopy (EM) on days 0, 7, and 14, at both pH 7.5 and 3.5. At

pH 7.5, day 0 (Fig. 9a and Table 5), A β 42 showed mainly small, globular assemblies ranging in diameter from 9 to 47 nm. A few assemblies were seen that were oblong, with lengths ranging from 15 to 28 nm and diameter ranging from 8 to 23 nm. iA β 42

Table 2. Comparison of the collision cross-section data for A β 42, iA β 42 conversion, and Ac-iA β 42 at pH 7.4 in negative ion mode

System	Oligomer	A β 42		iA β 42 \rightarrow A β 42		Ac-iA β 42	
		Charge state	σ (\AA^2)	σ/n	σ (\AA^2)	σ/n	σ (\AA^2)
Monomers							
Solvent free	-3	635	635	657	657	652	652
Solution-like	-3	702	702	718	718	712	712
Dimers							
-5	1256	628	1282	641	1318	659	
-6	—	1587	743				
Tetramer	-10	2332	583	2384	596	2204	551
Hexamer	-15	2898	483	2970	495	3024	504
Dodecamer (H ₂)	-30	4307	359	4428	369	4440	370

displayed similar globular structures, but their size distribution was skewed toward larger sizes (diameters ranging from 30 to 73 nm). Ac-iA β 42 produced assemblies similar to those of A β 42.

At day 7, all three peptides had formed fibrils. A β 42 displayed short and long fibrils ranging in diameter from 6 to 13 nm. The iA β 42 fibrils were long and relatively uniform in structure, with diameter of 5–11 nm. Some fibrils appeared to comprise twisted filaments with pitches of \approx 120–180 nm (Fig. 9a, blue and red arrows). A small number of globular assemblies of diameter 9–16 nm also were present.

Ac-iA β 42, in contrast to the other two peptides, formed a structurally heterogeneous population comprising predominately relatively straight fibrils with diameters of \approx 5–11 nm and lengths ranging from \approx 50 to 200 nm. At day 14, dense meshes of fibrils were formed by each of the peptides.

Analogous experiments were performed at pH 3.5 (Fig. 9b and Table 5). A β 42 formed short, often worm-like, structures at day 0. Globular or oblong structures also were observed. iA β 42, in contrast, formed predominately globular structures, similar to but of lesser diameter than those formed at pH 7.5.

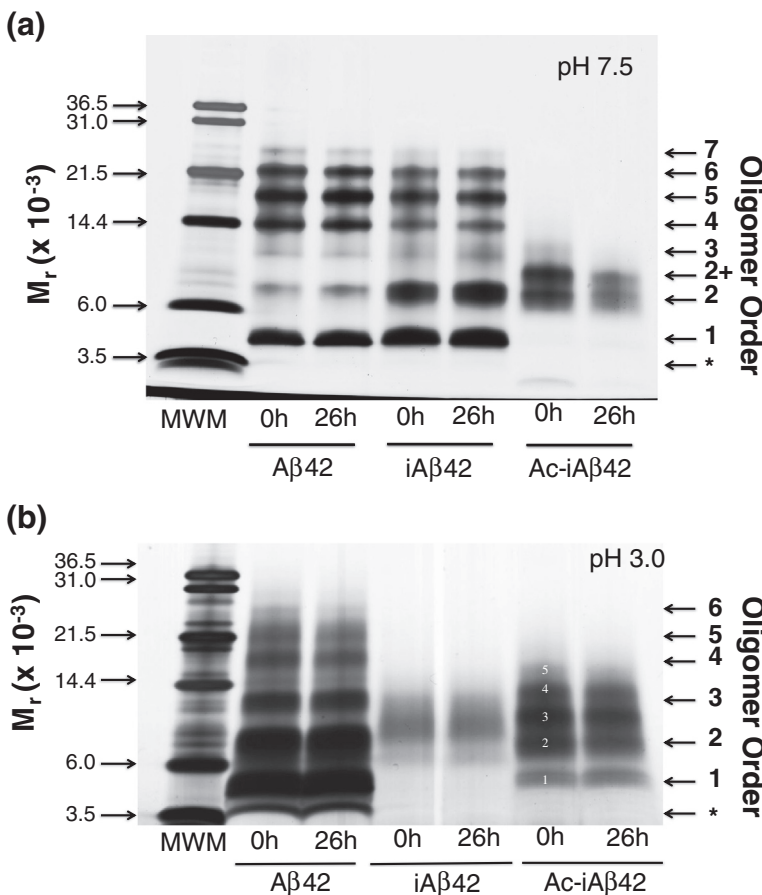


Fig. 8. Photochemical cross-linking. Oligomer distributions of A β 42, iA β 42, and Ac-iA β 42 were determined using PICUP, SDS-PAGE, and silver staining at the start of incubation at RT and after 26 h of incubation. (a) pH 7.5; (b) pH 3.0. A β 42, iA β 42, and Ac-iA β 42 were dissolved at a concentration of 1 mg/ml in pH 7.5 or pH 3.0 buffer. The samples were filtered using YM-50 Centricon (pH 7.5) and or Anotop 0.2- μ m filter (pH 3.0) and incubated at RT for 0 and 26 h. At each time point, an aliquot of the reaction was removed and cross-linked and samples analyzed on a 10–20% Tricine gradient gel followed by silver staining. Densitometric analysis of the gels was performed using Image J. Arrows on the right indicate oligomer order within the A β 42 lanes. The asterisk in (a) and (b) signifies the position of a band with an apparent molecular mass $<$ 3.5 kDa. In (b), white numbers overlaying bands in the Ac-iA β 42 lanes indicate nominal oligomer order for these specific bands.

Table 3. Densitometric analysis of the silver stained SDS-PAGE gel following PICUP at pH 7.5 using Image J

Oligomer order (<i>n</i>)	A β 42		iA β 42		Ac-iA β 42	
	0 h	26 h	0 h	26 h	0 h	26 h
1	19.4	21.2	23.1	22	2.1 ^a	3.5 ^a
2	13.1	13.4	25	25.6	38.4	49.1
2+	NP	NP	NP	NP	38.4	42.7
3	5.9	7.3	7.8	12.7	13.2	2.6
4	20.6	19.4	12.4	11.3	3.5	NP
5	21.9	20.8	18.3	15	NP	NP
6	14.7	14.7	11.3	11	NP	NP
7	4.2	3.2	2.0	2.4	NP	NP

The area of each band in a particular lane was normalized by the division of the sum of the areas of all the bands in that particular lane. This quotient was multiplied by 100 to yield the percentages in the table. Oligomer orders 1–7 in the table refer to monomer through heptamer. Areas of bands electrophoresing at the position of the asterisk were not quantified (see the main text). NP refers to Not Present.

^a These percentages represent the amount of the band electrophoresing just above the bottom of the gel (seen clearly in the 0 h lane).

Occasionally, a short, straight, or curved fibril was seen. Ac-iA β 42 formed a heterogeneous population of assemblies that included globular or oblong structures and numerous short, usually curved, fibrils.

At day 7, fibrils were observed in each peptide population. A β 42 formed predominately long fibrils, but with some short fibrils and globules as well. iA β 42 fibrils comprised two populations, one thicker (13–26 nm) than the other (3–8 nm). Ac-iA β 42 formed numerous short fibrils of variable length and some small globules.

At day 14, A β 42 fibril morphology remained similar to that at day 7. iA β 42 displayed a more heterogeneous population of fibrils than that observed at day 7. Both short and long fibrils were seen, and bright

small globules often were found associated with them. Whether these globules were an intrinsic part of the fibril structure, or simply adherent to the fibrils, cannot be ascertained. Ac-iA β 42 formed fibrils similar to those of iA β 42, although the average fibril length appeared shorter and the electron bright globules were more numerous and found both associated with and not associated with fibrils. There was greater heterogeneity among the assemblies formed by Ac-iA β 42 relative to those formed by A β 42 or iA β 42.

Discussion

The etiology of AD remains enigmatic. However, a number of viable working hypotheses exist, including those focusing on the role(s) of A β oligomers (reviewed in Refs. [4,33], and [34]). In the work reported here, we studied a region of the A β molecule thought critical in controlling monomer folding, oligomerization, and higher-order assembly, namely Ala21-Glu22-Asp23-Val24-Gly25~Ser26-Asn27-Lys28-Gly29-Ala30 [the tilde (~) signifies either an ester or a peptide bond] [6,10]. The tetrapeptide segment Gly25~Ser26-Asn27-Lys28 forms a turn-like structure stabilized by an extensive hydrogen bond network involving Ser26 [5–10]. This turn nucleates A β monomer folding [10], affects APP processing [12–15], and is a site for amino acid substitutions causing familial AD and CAA [6,9,11]. We used seven complementary methods, in two different pH regimes, to study the structural dynamics and assembly of A β 42 peptides containing a peptide (A β 42), an ester (iA β 42), or an N^α-acetyl ester (Ac-iA β 42) Gly25~Ser26 inter-amino acid bond. We also were able to examine the behavior of “nascent” A β 42 formed quasi-synchronously ($t_{1/2} \approx 30$ s) *in situ* through O → N acyl migration within iA β 42.

In discussing our results, we abstract key points from the large data set obtained, consider the significance of these points to *in vitro* studies of A β structural biology, and opine on how the data contribute to our understanding of the molecular pathogenesis of AD.

We found, as expected, that pH-induced O → N acyl migration in iA β 42 occurs rapidly, with a $t_{1/2} \approx 30$ s. The iA β 42 → A β 42 conversion thus is quasi-synchronous relative to the time constants for peptide secondary structure changes, oligomerization, or fibril formation, which are measured in hours and days. The rapid conversion allowed us to monitor structural features and dynamics of A β 42 monomers created *ab initio* *in situ*, a capability that avoids much of the confounding effects of A β peptide lyophilizate solvation and preparation for assay, for example, pre-existing β-sheets and intra-preparation aggregation [35].

Table 4. Densitometric analysis of the silver stained SDS-PAGE gel following PICUP at pH 3.0 using Image J

Oligomer order (<i>n</i>)	A β 42		iA β 42		Ac-iA β 42	
	0 h	26 h	0 h	26 h	0 h	26 h
*	6.5	8.0	NP	NP	NP	NP
1	21.7	21.8	20.1	21.9	17.3	18.2
2	25.9	28.0	59.4	58.6	28.4	29.0
3	20.9	18.3	20.5	19.4	29.1	29.0
4	11.7	13.4	NP	NP	18.4	18.8
5	10.5	9.0	NP	NP	6.8	4.8
6	2.5	1.3	NP	NP	NP	NP
7	0.2	0.3	NP	NP	NP	NP

The area of each band in a particular lane was normalized by the division of the sum of the areas of all the bands in that particular lane. This quotient was multiplied by 100 to yield the percentages in the table. Oligomer orders 1–7 in the table refer to monomer through heptamer. NP refers to Not Present.

We observed a remarkable agreement among data from experiments monitoring rates of increase in β -sheet formation (ThT, CD), R_H , and scattering

intensity (QLS). This kinetics showed a rank order of Ac-iA β 42 > iA β 42 > A β 42. Why? A reasonable supposition is that the rank order reflects the relative

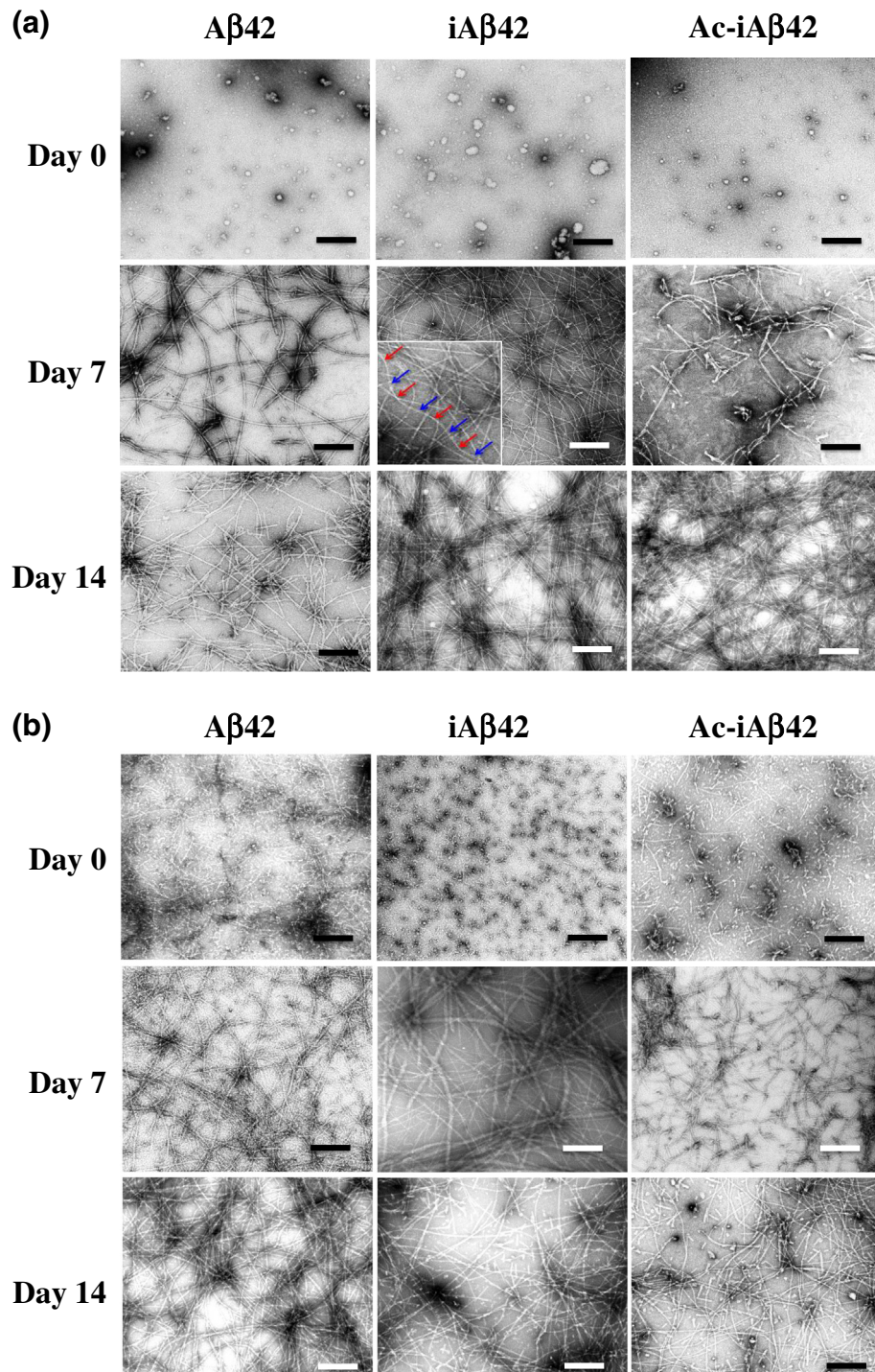


Fig. 9. Morphology of A β assemblies. EM of A β 42, iA β 42, and Ac-iA β 42 was performed after 0, 7, and 14 days of assembly at (a) pH 7.5 or (b) pH 3.5. Inset in (a) is a magnified region. Fibril twisting is noted by red arrows (narrow or on-edge structure) and blue arrows (wide, multi-filar structures). Scale bars are 200 nm.

Table 5. Dimensions of assemblies observed by EM

Peptide	pH	Day 0			Day 7			Day 14		
		Globules	Short fibrils	Long fibrils	Globules	Short fibrils	Long fibrils	Globules	Short fibrils	Long fibrils
A β 42	7.5	9–47 8–23 (15–28)	—	—	—	6–13 (117–178)	6–13	—	9–12 (33–157)	7–12
iA β 42	7.5	12–56	—	—	9–16	5–11	5–11	8–30	—	5–14
Ac-iA β 42	7.5	11–36	—	—	7–12 10–14 (36–73)	5–8 (52–208)	6–11	—	—	4–8
A β 42	3.5	(15–35)	5–12	—	—	—	6–13	—	—	5–11
iA β 42	3.5	(17–47)	—	—	—	—	3–8 13–26	—	—	5–11
Ac-iA β 42	3.5	4–8	5–10 (17–66)	6–10 (82–239)	5–14	7–11 (34–366)	5–9	9–15 12–32 (21–52)	7–9 (42–78)	5–8

Peptides were incubated at either pH 7.5 or 3.5. Following incubation, we observed different classes of assemblies, including globules, short fibrils, and long fibrils. If present, the numbers represent the size range, in units of nanometers, of each assembly type. Assembly lengths are reported in parentheses.

abilities of each peptide to fold and self-associate into ordered (in this case, β -sheet-rich) assemblies. Ac-iA β 42 could display a greater area of solvent-accessible hydrophobic surface due to a lower propensity to form the Gly25-Lys28 turn, which prevents intramolecular interactions between hydrophobic peptide segments adjacent to the turn (the “legs” in a β -hairpin). The result would be a concomitant increase in intermolecular interactions among these exposed hydrophobic regions and a rapid hydrophobic collapse producing either off-pathway aggregates or molten globule-like structures. In the former case, conversion to ordered oligomers or fibrillar structures would not occur, whereas in the latter case, ordered assembly into higher-order structures, including protofibrils and fibrils, might be facilitated (Fig. 10).

This latter argument is consistent with the increased rate of conformational change in the iA β 42 sample. A reasonable supposition is that the rate difference between iA β 42 and A β 42 is due to the conversion of iA β 42 into “pure” A β 42 monomer, that is, nascent A β 42 that exists as a monomer, absent pre-existent “off-pathway” aggregates that could retard movement along the pathway of oligomers \rightarrow protofibrils \rightarrow fibrils (Fig. 10). The idea of a nascent A β monomer, as discussed above, may explain why limited proteolysis experiments at pH 2 demonstrated a rank order of protease sensitivity of iA β 42 $>$ A β 42 \approx Ac-iA β 42. Among the three peptides, iA β 42 is least able to fold/collapse to sequester protease-sensitive peptide bonds. Results at pH 7.5 are also consistent with this proposition. In this pH regime, where iA β 42 converts rapidly to A β 42 and where protease action is very rapid, similar proteinase K digestion sensitivities were observed for the two peptides. In contrast, Ac-iA β 42 was significantly ($p < 0.005$) less sensitive to proteinase K than were A β 42 or iA β 42, likely due to rapid aggregation (as was shown in QLS studies), which sequestered pepsin-sensitive peptide bonds.

IMS-MS experiments were particularly useful in monitoring the oligomerization phases of A β assembly. Injection energy-dependent ion mobility spectroscopy studies revealed both the existence and stabilities of different oligomers. ATDs of the $-5/2$ (z/n) ions of A β 42 and iA β 42 differed. This was particularly true of the ATDs acquired at low injection energies (23 eV and 30 eV for A β 42 and iA β 42, respectively). Only di-hexamer and hexamer were observed in the A β 42 sample, whereas di-hexamer, tetramer, and dimer were observed with iA β 42. The ATDs at 50 eV showed that the di-hexamers and di-pentamers formed from nascent A β 42 were more prominent than those formed by pre-existent A β 42. This observation was consistent with the ATDs of the -3 ions of each isoform, which demonstrated that converted iA β 42 forms stable dimers at 30 eV injection energy whereas A β 42 does not. Taken together, these data are consistent with our

prior supposition that nascent A β 42 (i.e., iA β 42 immediately after pH-induced conversion to A β 42) exists in a monomer state that more readily forms low-order oligomers than does A β 42, which exists *ab initio* in a variety of oligomeric and aggregated states. It should be noted that our data also are consistent with the formation of mixed iA β 42/A β 42 dimers in the -6 and -5 charge states, and these mixed systems may contribute to formation of higher-order oligomers in the iA β 42 system at high pH. This may be so because dimerization of iA β 42 and nascent A β 42 occurs intra-experimentally before iA β 42 is able to convert completely to A β 42.

In the case of Ac-iA β 42, the very poorly resolved mass spectrometry spectra suggested that substantial aggregation occurred rapidly following sample dissolution in 10 mM buffer. This hypothesis was confirmed by study of the same peptide in 100 μ M buffer (a 100-fold lower buffer concentration), a concentration regime in which well-resolved spectra were produced that had predominant peaks at *m/z* values of -4, -3, and -5/2, similar to those produced by iA β 42. ATD experiments on the -5/2

ion of Ac-iA β 42 acquired at an injection energy of 50 eV displayed a peak distribution comprising di-hexamer and di-pentamer, as did those of A β 42 and iA β 42 samples, but also a much more intense hexamer peak and essentially no dimer peak. These data are consistent with the fact that this isoform aggregates much faster than either A β 42 or iA β 42. The high aggregation propensity of Ac-iA β 42 observed in the IMS-MS experiments was consistent with the high assembly/aggregation propensities observed in the prior ThT, CD, QLS, and proteolysis experiments.

The IMS-MS data confirm and extend the observation of assembly differences between pre-existent A β 42 and nascent A β 42 (formed from conversion of iA β 42). As mentioned above, these differences could involve formation of mixed dimers of the two isoforms. Another possibility is that conversion of the iA β 42 to A β 42 produces a much more homogeneous population of A β 42 monomers, as opposed to a pre-existent A β 42 population that already contains monomers, oligomers, and aggregates. This monomer population self-associates through a smaller

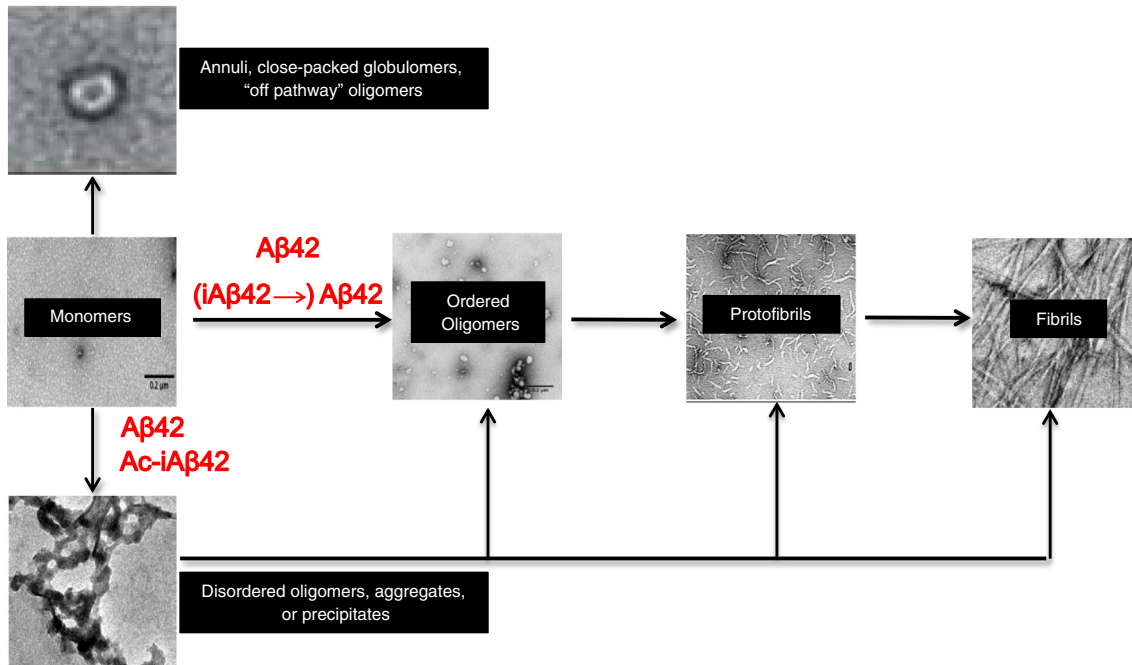


Fig. 10. Pathways of A β assembly. The assembly of A β into fibrils (“on pathway”) may follow a linear pathway from A β monomer to oligomer to protofibril to fibril [4]. Monomers may assemble into a variety of non-fibrillar structures, including annuli (pores) [36], quasi-spherical or oblong structures, close-packed globules, and “off-pathway” oligomers. Monomers also may aggregate into relatively amorphous structures the size of oligomers or into larger aggregates or precipitates. These aggregates may undergo structural rearrangement and reenter the pathway of fibril formation. iA β 42 converts into nascent A β 42 that has a high propensity for dimerization and facile entry and movement down the fibril formation pathway. A β 42, depending on its starting assembly states, may form off-pathway assemblies or also traverse the fibril formation pathway. Ac-iA β 42 appears first to undergo rapid aggregation followed by structural reorganization and eventual fibril formation. [The annulus in the figure is reprinted by permission from Macmillan Publishers Ltd: *Nature Protocols* (Vol. 5: No. 6: 1186–1209), copyright (2010).]

number of pathways relative to pre-existent A β 42, which forms a much more heterogeneous population of conformers and pre-existent oligomers and thus accesses a more diverse set of assembly paths and products. The effects of starting state conformation are even more pronounced with the Ac-iA β 42 peptide. The acetylation of this peptide eliminates the possibility of native-like folding at Gly25 and Ser26 resulting in rapid aggregation, potentially due to the enthalpic gains of sequestering solvent-exposed hydrophobic peptide regions or establishing Coulombic or hydrogen bond interactions (Fig. 10).

We used PICUP as one orthogonal method for determining A β oligomerization state. iA β 42 converts to A β 42 during PICUP experiments performed at pH 7.5. The experiment thus reveals features of the oligomer distribution of nascent A β 42, that is, a population of peptides initially comprising monomeric A β 42. When iA β 42 was cross-linked, the most striking feature of the oligomer distribution, relative to pre-existent A β 42, was an intense dimer band. Fewer tetramers and hexamers were observed, a result consistent with the “zero sum” nature of the system—namely, increases in dimer concentration had to be compensated for by decreases in the concentrations of other oligomers. The existence of higher numbers of dimers is consistent with the existence of greater numbers of monomers after conversion (through the law of mass action). This contrasts with pre-existent A β 42, which has been shown to contain β -sheet structures even in its lyophilized state [35] and thus presents what one might conceptualize as a partially “pre-aggregated” state. As discussed above, a prominent \sim 6 dimer was also observed in the IMS–MS experiments with iA β 42 (Fig. 7a), but not for A β 42.

Ac-iA β 42 displayed a strikingly different pH 7.5 oligomer distribution, one characterized by essentially a single feature, two bands migrating with apparent molecular weights slightly lower and slightly higher, respectively, than that of A β 42 dimer. The narrow distribution of oligomers is consistent with the SDS-induced dissociation of large Ac-iA β 42 aggregates, such as those observed in QLS and IMS–MS experiments. Rapid aggregation could sequester sites of cross-linking, explaining why A β 42-like oligomer distributions were not observed.

Oligomer distributions in PICUP experiments at pH 3.0 were instructive. The “ladder-type” distribution of A β 42 (monotonic decrease in band intensity) was consistent with simple diffusion-limited peptide:peptide interactions, in contrast to the discontinuous distribution characteristic of normal A β 42 oligomerization. Nevertheless, the presence of bands up to the size of heptamer shows that the oligomer organization necessary for successful intermolecular cross-linking existed in A β 42 at this pH. This was not the case with

iA β 42, which displayed a single predominant band migrating between dimer and trimer (along with a faint band migrating between monomer and dimer). This distinct pattern, and the absence of a monomer band, suggests highly efficient cross-linking of a single predominant oligomer form and, by inference, the inability of the Gly25-Ser26 peptide ester to assume a conformation characteristic of the normal, peptide-bond-containing A β 42 isomer. It is possible that this predominant form is the dimer found so abundantly in IMS–MS work. The fundamental conformational basis for this cross-linking difference could be that monomers at pH 3.0 rapidly form dimers with adjacent Tyr10 residues. It also is possible that higher-order oligomers existed but were not cross-linked, as evidenced by the lack of SDS-stable higher-order oligomer bands. A related mechanism could explain the broader distribution of Ac-iA β 42 oligomer types observed at pH 3.0 *versus* pH 7.5—whether as specific oligomers or as oligomers within much larger assemblies, chemical accessibility is higher at pH 3.0 and thus a broader range of covalently associated (SDS-stable) oligomers is observed.

Finally, and not surprisingly, differences observed among the peptides in oligomerization (IMS–MS, PICUP), assembly kinetics (QLS, CD), β -sheet formation (ThT fluorescence and CD), and protease sensitivity were reflected in quaternary structure variations determined by EM. All peptides formed globular structures and fibrils, but the relative amounts of each of these structures, and their precise morphologies, differed depending on pH and time.

Conclusions

We observed a remarkable agreement among data from experiments monitoring β -sheet formation (ThT, CD), hydrodynamic radius (R_H) and scattering intensity (QLS), and oligomerization (IMS–MS), namely a rank order of Ac-iA β 42 > iA β 42 > A β 42. These data were consistent with high protease resistance of Ac-iA β 42. When iA β 42 was cross-linked, the most striking feature of the oligomer distribution, relative to pre-existent A β 42, was an intense dimer band. IMS–MS experiments also showed that pre-existent A β 42 did not form stable dimers, whereas iA β 42 did, a fact that could explain why this latter peptide could also readily form dodecamers and decamers. Effects of Gly25-Ser26 structure were reflected in the constellations of quaternary structures determined by EM. The distinct biophysical behaviors of iA β 42 and A β 42 appear to be due to the conversion of iA β 42 into nascent (pure) A β 42 monomer, which lacks the variety of oligomeric and aggregated states present in pre-existent A β 42. It is intriguing to consider whether *in situ* creation of A β 42 from iA β 42 in biological systems might yield results distinct from those obtained using preformed A β 42 and thus

challenge prevailing views of A β 42 structure–activity relationships. In conclusion, our results emphasize the importance of the Gly25-Ser26 dipeptide in organizing A β 42 monomer structure and thus suggest that drugs altering the interactions of this dipeptide with neighboring side-chain atoms or with the peptide backbone could be useful in therapeutic strategies targeting formation of A β oligomers and higher-order assemblies. Recent studies showing that iA β 42 (at pH 2) and [N $^{\alpha}$ -methyl- β -Ala26]A β 42 (at pH 7.4) do indeed inhibit fibril formation augur well for this strategy [37].

Materials and Methods

Chemicals and reagents

All chemicals and enzymes were purchased from Sigma Chemical Co. (Saint Louis, MO) and were of the highest purity available. Water was de-ionized and filtered using a Milli-Q system (Millipore Corp., Bedford, MA). YM-50-kDa filters were purchased from Millipore Corp. XpressTM silver-staining kit was from Invitrogen (Carlsbad, CA). Solvents for liquid chromatography–mass spectrometry were HPLC grade (Fisher Scientific, Pittsburgh, PA).

Peptide synthesis

iA β 42, 26-N $^{\alpha}$ -acetyl-*O*-acyliso-A β 42 (Ac-iA β 42), and A β (1–42) (A β 42) were synthesized using 9-fluorenylmethoxycarbonyl (Fmoc) chemistry and purified by RP-HPLC, essentially as described previously [38]. The identity and purity (usually >97%) of the peptides were confirmed by amino acid analysis, mass spectrometry, and RP-HPLC. Ac-iA β 42 was synthesized as described above, except that Fmoc-Ser-OH, not Fmoc-Ser(tBu)-OH, was coupled to Asn27. Following coupling and washing with NMP, the Fmoc group of serine was removed with 20% (v/v) 4-methyl piperidine in NMP by incubating for 20 min at RT (23 °C). Acetylation of the Ser N $^{\alpha}$ atom was accomplished using 0.5 M acetic anhydride, 0.125 M DIEA, and 0.15 M HOBt in NMP. Following washing in NMP, we coupled Fmoc-Gly-OH then to the Ser 26 OH $^{\beta}$ using the DIPCDI-DMAP method, as per Sohma *et al.* [19].

Kinetics of production of A β 42 from iA β 42

Lyophilizates of A β 42, iA β 42, or Ac-iA β 42 were dissolved immediately prior to assay by gentle vortexing at concentrations of 20–30 μ M in 100 mM ammonium bicarbonate, pH 8.0. Peptides were incubated at RT without agitation. Eight-microliter aliquots of the reaction volume were removed periodically and added to 5 μ L of trifluoroacetic acid (TFA) (to stop conversion of the iA β 42 peptide samples). The samples then were placed on ice. Ten microliters of HPLC solvent A [2% (v/v) acetonitrile, 0.1% (v/v) acetic acid, and 0.02% (v/v) TFA, in water] was added to the sample and the mixture then was analyzed by RP-HPLC. A 2–100% gradient of solvent B [acetonitrile in 0.1% (v/v) acetic acid and 0.02% (v/v) TFA] was run over a

40-min time period using a C₁₈ column (Nova-Pak 3.9 mm × 150 mm, 4 mm particle size, 60 Å pore size) eluted at a flow rate of 1 ml/min with UV peak detection at 215 nm [10,39]. Peak Simple 2000 Chromatography Integration Software (SRI Instruments, Torrance, CA) was used to determine peak areas in the resulting chromatograms.

ThT binding

Peptides were prepared at a nominal concentration of 0.5–1 mg/ml by dissolving lyophilizates in 1 volume of 60 mM NaOH:4.5 volumes of milliQ water:4.5 volumes of 20 mM sodium phosphate buffer, pH 7.5, containing 0.002% (w/v) sodium azide. The solutions were sonicated for 1 min in a Branson 1200 bath sonicator (Branson Ultrasonics Corp., Danbury, CT). The peptide solutions then were centrifuged in a pre-wetted YM-50 kDa filter at 16,000*g* for 10 min. The pH of the peptide solutions was confirmed using a micro pH electrode (Orion, Model 9810BN). After centrifugation and filtering, we determined the concentration of the peptides from their A_{280} values, using an extinction coefficient of 1280 cm^{−1} M^{−1}.

Assays were conducted in 0.4-ml, 96-well, optical bottom, polymer-based microtiter plates (Thermo Scientific Nunc, Rochester, NY). An aliquot of the A β 42 stock solution (see above) was pipetted into each well, followed by 1.6 μ L of 5 μ M ThT in phosphate buffer. The total volume in each well was adjusted to 200 μ L with phosphate buffer, yielding a final A β concentration of 20 μ M and a ThT concentration of 40 μ M. The wells were gently mixed by pipetting, sealed using an adhesive plate sealer, and incubated at 37 °C with gentle shaking. The plate was read in a microplate reader ($\lambda_{\text{ex}} = 450$ nm, $\lambda_{\text{em}} = 482$ nm) immediately and then at regular intervals. Blank wells contained ThT and buffer. Five or more replicates were performed for each sample. The mean of the blank readings was subtracted from the mean of the sample readings at each time point and the corrected values, along with SD and mean, were plotted using KaleidaGraph (v4.1, Synergy Software, Reading, PA). Statistical analyses on the data (*t*-test and Mann–Whitney Rank test) were performed using SigmaStat (Jandel Scientific, San Jose, CA).

QLS spectroscopy

In experiments at neutral conditions, A β 42, iA β 42, and Ac-iA β 42 were dissolved at a nominal concentration of 0.5 mg/ml (110 μ M) in 20 mM sodium phosphate, pH 7.5, briefly vortexed, sonicated for 20 s, and filtered using a 20-nm Anotop filter (Whatman International Ltd., Maidstone, England). Amino acid analysis was performed *post facto* to determine the actual protein concentration (see Results). Samples were monitored at RT for 7–10 days. In experiments with initial acidic conditions, samples of iA β 42 and Ac-iA β 42 were dissolved in 0.2 mM sodium acetate, pH 3.5, at concentrations of 77 μ M and 154 μ M, respectively. Each sample then was vortex mixed briefly, sonicated for 20 s, and filtered using a 20-nm Anotop filter. Samples were monitored at RT for 3 days and then brought to neutral pH by addition of 0.5 volume of 20 mM sodium phosphate, pH 7.5. Measurements were performed using a custom optical setup comprising a 40 mW He-Ne laser ($\lambda = 633$ nm) (Coherent, Santa Clara, CA) and PD2000DLS detector/

correlator unit (Precision Detectors, Bellingham, MA). Light scattering was measured at a 90° angle. The intensity correlation function and the diffusion coefficient (D) frequency distribution were determined using Precision Deconvolve software (Precision Detectors, Bellingham, MA). The hydrodynamic radius R_H was calculated from D according to the Stokes-Einstein equation, $D = \frac{k_B T}{(6\pi\eta R_H)}$, where k_B is Boltzmann's constant, T is Kelvin, and η is the solvent viscosity [40].

Limited proteolysis

Peptides (2 mg/ml) were digested using proteinase K or porcine pepsin. Proteinase K digestions were performed by adding the enzyme, at an enzyme:substrate ratio of 1:1000 (w/w), to A β dissolved in 100 mM ammonium bicarbonate, pH 8.0, after addition of 10% (v/v) 60 mM NaOH. Aliquots were removed at 0, 15, and 90 min, and then the reactions were quenched using 20 μ l of 50% (v/v) TFA in water.

Pepsin digestion was performed by adding the enzyme to peptides dissolved directly in 10 mM HCl, pH 2.0, at an enzyme:substrate ratio of 1:1000 (w/w). Digestion was allowed to proceed at RT for 0, 15, or 90 min. At each time point, a 20- μ l aliquot was removed and the proteolysis was stopped by addition of 10 μ l of 5% (v/v) ammonium hydroxide in water.

The resulting samples were analyzed by gradient RP-HPLC using a Nova-Pak 3.9 mm × 150 mm, 4 mm particle size, 60 Å pore size, C₁₈ column. Solvent A was 0.02% (v/v) TFA, 0.1% (v/v) acetic acid, and 2% acetonitrile (v/v) in water. Solvent B was 90% (v/v) acetonitrile, 0.02% (v/v) TFA, and 0.1% (v/v) acetic acid, in water. A linear (1.25% B/min) gradient from 0% to 100% B was run at a flow rate of 1.0 ml/min. Peak detection was performed by UV absorbance at 215 nm. Peak quantitation was performed using Peak Simple 2000 Chromatography Integration Software. Statistical analyses on the data (*t*-test and Mann-Whitney Rank test) were performed using SigmaStat.

CD spectroscopy

A β 42, iA β 42, and Ac-iA β 42 peptide solutions were prepared as stated in ThT binding. The peptides then were incubated at 37 °C with gentle shaking in an Innova 4080 incubator shaker (New Brunswick Scientific, Edison, NJ). CD spectra were obtained every 30 min for the first 2 h, and subsequently every hour, using a JASCO J-810 spectropolarimeter (Tokyo, Japan). The CD parameters were as follows: wavelength scan range, 190–260 nm; data pitch, 0.2 nm; continuous scan mode, 10 scans of each sample; scan speed, 100 nm/min; response, 1 s; and band width, 2 nm. The spectra were processed using the means movement smoothing parameter within the Spectra Manager software. The data were subsequently plotted using KaleidaGraph (v4.1.3).

Ion mobility spectrometry-mass spectrometry

Standard mass spectra and ion mobility experiments were performed on an instrument built “in-house” that

comprises a nano-electrospray ionization (N-ESI) source, an ion funnel, a temperature-controlled drift cell, and a quadrupole mass filter followed by an electron multiplier for ion detection [41]. The high-resolution ¹³C isotope distributions for each peak in the mass spectra were obtained on a Q-TOF mass spectrometer (Micromass, UK) equipped with an N-ESI source [42,43]. During ion mobility measurements, the ions were stored at the end of the ion funnel and then pulsed into the drift cell, which was filled with 5 Torr of helium gas, and drawn through the cell under the influence of a weak electric field (2–20 V/cm). The ion injection energy into the drift cell was varied from 20 to 100 eV. At low injection voltages, the ions were gently pulsed into the mobility cell and only needed a few “cooling” collisions to reach thermal equilibrium with the buffer gas helium. At high injection voltages, the larger collision energy led to internal excitation of the ions before cooling and equilibrium occurred. This transient internal excitation can lead to annealing, that is, partial or complete isomerization, to give the most stable conformers or can lead to dissociation of dimers and oligomers of higher order [30]. The ions exit the drift cell and pass through a quadrupole mass filter, allowing a mass spectrum to be obtained. Alternatively, the quadrupole can be set to monitor a specific peak in the mass spectrum as a function of time, producing an ATD. The arrival time is related directly to the mobility constant K , which in turn is inversely proportional to the collision cross-section σ [43,44]. Accurate ($\pm 1\%$) collision cross-sections are obtained.

All A β 42 samples were dissolved at 1 mg/ml (0.22 mM) in 25 mM ammonium acetate, pH 8.3, resulting in a final pH of 7.4. Immediately prior to mass spectrometry analysis, the stock solution was diluted to 20 μ M in 25 mM ammonium acetate (or other desired buffer concentrations) and adjusted to the appropriate pH for the experiment. A 5- to 10- μ l aliquot of sample was loaded into a metal-coated borosilicate glass capillary for N-ESI applications.

Oligomerization of A β 42

A β oligomerization was monitored using PICUP, essentially as described previously [45]. Peptide solutions at pH 7.5 were prepared essentially as stated in ThT binding. Peptide solutions at pH 3.0 were prepared by dissolving lyophilizates directly in 0.1 M glycine-HCl, pH 3.0, at concentrations 0.5–1 mg/ml. The solutions were sonicated for 1 min in a Branson 1200 bath sonicator (Branson Ultrasonics Corp.), after which they were filtered using a sterile 0.20- μ m Anotop filter (Whatman International Ltd.). The peptides then were incubated at RT.

Eighteen microliters of sample were periodically cross-linked using the PICUP reaction [46]. Briefly, 1 μ l of 2 mM Tris (2,2'-bipyridyl) dichlororuthenium (II) hexahydrate [Ru(bpy)] was added to a 0.2-ml thin-walled PCR tube (Eppendorf AG, Hamburg, Germany) containing the sample, followed by addition of 1 μ l of 40 mM ammonium persulfate in phosphate-buffered saline. The tube then was irradiated for 1 s with incandescent light using a high-intensity illuminator (Model 170-D; Dolan-Jenner Industries Inc.). The reaction was quenched immediately with 1 μ l of 1 M DTT in water and the sample was vortexed and placed on ice. To determine the oligomer size distribution, we added an equal volume of 2×

Tris-N-[2-hydroxy-1,1-bis(hydroxymethyl)ethyl]glycine (Tricine) SDS sample buffer (Invitrogen) to each sample. The samples then were boiled in a 100 °C water bath for 5–10 min and electrophoresed on a 10–20% T (1 mm thick) Tris-Tricine SDS gel (Invitrogen). The gel was silver stained using a SilverXpress® Silver Staining Kit (Novex). For cross-linking at pH 3.0, all reagents were dissolved directly in 0.1 M glycine-HCl, pH 3.0. The PICUP chemistry occurs at pH 3.0 as it does at other pH values [32].

Electron microscopy

Formvar 400-mesh grids were glow discharged on a Med010 mini-deposition system EM glow discharge attachment (model BU007284-T; Balzers Union Ltd., Hudson, NH) containing a cylindrical discharge compartment and an adjacent discharge control and timer unit. Samples were mixed thoroughly and then 8 μ l was applied onto the grid. The grid was covered and incubated for 20 min at RT. Liquid was wicked off using a filter paper wick by gently touching the tip of the filter paper to the edge of the grid. Five microliters of 2.5% (v/v) glutaraldehyde in water were applied to the grid, which was incubated for 3 min in the dark. The glutaraldehyde solution was wicked off and replaced with 5 μ l of 1% (w/v) uranyl acetate in water and was incubated for 3 min in the dark. The grids then were wicked off and air-dried. A JEOL 1200 EX (JEOL Ltd., Tokyo, Japan) transmission electron microscope was used to visualize the samples.

Supplementary data to this article can be found online at <http://dx.doi.org/10.1016/j.jmb.2014.04.004>.

Acknowledgements

This work was supported by National Institutes of Health Grants NS038328 (D.B.T.), AG047116 (M.T.B.), and AG041295 (D.B.T.) and by the Jim Easton Consortium for Drug Discovery and Biomarkers at University of California Los Angeles (D.B.T.). We acknowledge the use of instruments at the Electron Imaging Center for NanoMachines at the California NanoSystems Institute, University of California Los Angeles (supported by National Institutes of Health Grant 1S10RR23057). Waters Corp is also acknowledged for the donation of a prototype Synapt TWIMS spectrometer (to M.T.B.).

Received 12 February 2014;

Received in revised form 7 April 2014;

Accepted 8 April 2014

Available online xxxx

Keywords:

amyloid β -protein;
Alzheimer's disease;
ion mobility spectroscopy–mass spectrometry;
oligomerization;

[†]We define lag phase as the period between initial sample preparation/monitoring and the beginning of continuous increases in intensity. This time is determined by establishing the point of intersection of two lines, one fitted to the initial quasi-constant intensity portion of the progress curve and the other one fitted to that portion in which persistent increases in intensity are observed. This latter curve fit also is used to establish dRH/dt.

Abbreviations used:

$\text{A}\beta$, amyloid β -protein; AD, Alzheimer's disease; ATD, arrival time distribution; RP-HPLC, reverse-phase high-performance liquid chromatography; IMS–MS, ion mobility spectroscopy–mass spectrometry; PICUP, photo-induced cross-linking of unmodified proteins; QLS, quasielastic light scattering; ThT, thioflavin T; TFA, trifluoroacetic acid; N-ESI, nano-electrospray ionization; Tricine, N-[2-hydroxy-1,1-bis(hydroxymethyl)ethyl]glycine.

References

- [1] Selkoe DJ. Biochemistry and molecular biology of amyloid β -protein and the mechanism of Alzheimer's disease. *Handb Clin Neurol* 2008;89:245–60.
- [2] Goedert M, Spillantini MG. A century of Alzheimer's disease. *Science* 2006;314:777–81.
- [3] Hardy J, Selkoe DJ. The amyloid hypothesis of Alzheimer's disease: progress and problems on the road to therapeutics. *Science* 2002;297:353–6.
- [4] Roychaudhuri R, Yang M, Hoshi MM, Teplow DB. Amyloid β -protein assembly and Alzheimer disease. *J Biol Chem* 2009;284:4749–53.
- [5] Borreguero JM, Urbanc B, Lazo ND, Buldyrev SV, Teplow DB, Stanley HE. Folding events in the 21–30 region of amyloid β -protein ($\text{A}\beta$) studied *in silico*. *Proc Natl Acad Sci U S A* 2005;102:6015–20.
- [6] Grant MA, Lazo ND, Lomakin A, Condron MM, Arai H, Yamin G, et al. Familial Alzheimer's disease mutations alter the stability of the amyloid β -protein monomer folding nucleus. *Proc Natl Acad Sci U S A* 2007;104:16522–7.
- [7] Cruz L, Urbanc B, Borreguero JM, Lazo ND, Teplow DB, Stanley HE. Solvent and mutation effects on the nucleation of amyloid β -protein folding. *Proc Natl Acad Sci U S A* 2005;102:18258–63.
- [8] Baumketner A, Bernstein SL, Wyttenbach T, Lazo ND, Teplow DB, Bowers MT, et al. Structure of the 21–30 fragment of amyloid β -protein. *Protein Sci* 2006;15:1239–47.
- [9] Krone MG, Baumketner A, Bernstein SL, Wyttenbach T, Lazo ND, Teplow DB, et al. Effects of familial Alzheimer's disease mutations on the folding nucleation of the amyloid β -protein. *J Mol Biol* 2008;381:221–8.
- [10] Lazo ND, Grant MA, Condron MC, Rigby AC, Teplow DB. On the nucleation of amyloid β -protein monomer folding. *Protein Sci* 2005;14:1581–96.
- [11] Chen W, Mousseau N, Derreumaux P. The conformations of the amyloid- β (21–30) fragment can be described by three families in solution. *J Chem Phys* 2006;125:084911.
- [12] Ren Z, Schenk D, Basi GS, Shapiro IP. Amyloid β -protein precursor juxtamembrane domain regulates specificity of γ -secretase-dependent cleavages. *J Biol Chem* 2007;282:35350–60.

- [13] Sato T. A helix-to-coil transition at the ϵ -cut site in the transmembrane dimer of the amyloid precursor protein is required for proteolysis. *Proc Natl Acad Sci U S A* 2009;106:1421–6.
- [14] Bernstein SL, Dupuis NF, Lazo ND, Wyttenbach T, Condron MM, Bitan G, et al. Amyloid- β protein oligomerization and the importance of tetramers and dodecamers in the aetiology of Alzheimer's disease. *Nat Chem* 2009;1:326–31.
- [15] Lichtenthaler SF, Beher D, Grimm HS, Wang R, Shearman MS, Masters CL, et al. The intramembrane cleavage site of the amyloid precursor protein depends on the length of its transmembrane domain. *Proc Natl Acad Sci U S A* 2002;99:1365–70.
- [16] Mutter M, Chandravarkar A, Boyat C, Lopez J, Dos Santos S, Mandal B, et al. Switch peptides in statu nascendi: induction of conformational transitions relevant to degenerative diseases. *Angew Chem Int Ed Engl* 2004;43:4172–8.
- [17] Sohma Y, Kiso Y. “Click peptide”: chemical biology-oriented synthesis of Alzheimer's disease-related amyloid β peptide (A β) analogues based on the “O-acyl isopeptide method”. *ChemBioChem* 2006;7:1549–57.
- [18] Sohma Y, Sasaki M, Hayashi Y, Kimura T, Kiso Y. Novel and efficient synthesis of difficult sequence-containing peptides through O–N intramolecular acyl migration reaction of O-acyl isopeptides. *Chem Commun* 2004:124–5. <http://dx.doi.org/10.1039/B312129A>.
- [19] Sohma Y, Yoshiya T, Taniguchi A, Kimura T, Hayashi Y, Kiso Y. Development of O-acyl isopeptide method. *Biopolymers* 2007;88:253–62.
- [20] Teplow DB, Lazo ND, Bitan G, Bernstein S, Wyttenbach T, Bowers MT, et al. Elucidating amyloid β -protein folding and assembly: a multidisciplinary approach. *Acc Chem Res* 2006;39:635–45.
- [21] Teplow DB. Preparation of amyloid β -protein for structural and functional studies. *Methods Enzymol* 2006;413:20–33.
- [22] Hartley DM, Walsh DM, Ye CP, Diehl T, Vasquez S, Vassilev PM, et al. Protomeric intermediates of amyloid β -protein induce acute electrophysiological changes and progressive neurotoxicity in cortical neurons. *J Neurosci* 1999;19:8876–84.
- [23] Naiki H, Nakakuki K. First-order kinetic model of Alzheimer's β -amyloid fibril extension *in vitro*. *Lab Invest* 1996;74:374–83.
- [24] LeVine H. Quantification of β -sheet amyloid fibril structures with thioflavin T. *Methods Enzymol* 1999;309:274–84.
- [25] Groenning M. Binding mode of thioflavin T and other molecular probes in the context of amyloid fibrils—current status. *J Chem Biol* 2010;3:1–18.
- [26] Lomakin A, Benedek GB, Teplow DB. Monitoring protein assembly using quasielastic light scattering spectroscopy. *Methods Enzymol* 1999;309:429–59.
- [27] Lomakin A, Teplow DB, Benedek GB. Quasielastic light scattering for protein assembly studies. *Methods Mol Biol* 2005;299:153–74.
- [28] Lomakin A, Teplow DB. Quasielastic light scattering study of amyloid β -protein fibrillogenesis. *Methods Mol Biol* 2012;849:69–83.
- [29] Nomenclature E. IUBMB Enzyme Nomenclature: Pepsin. <http://www.chem.qmul.ac.uk>; 1989.
- [30] Bernstein SL, Wyttenbach T, Baumketner A, Shea J-E, Bitan G, Teplow DB, et al. Amyloid β -protein: monomer structure and early aggregation states of A β 42 and its Pro19 alloform. *J Am Chem Soc* 2005;127:2075–84.
- [31] Baumketner A, Bernstein SL, Wyttenbach T, Bitan G, Teplow DB, Bowers MT, et al. Amyloid β -protein monomer structure: a computational and experimental study. *Protein Sci* 2006;15:420–8.
- [32] Bitan G, Lomakin A, Teplow DB. Amyloid β -protein oligomerization: prenucleation interactions revealed by photo-induced cross-linking of unmodified proteins. *J Biol Chem* 2001;276:35176–84.
- [33] Benilova I, Karra E, De Strooper B. The toxic A β oligomer and Alzheimer's disease: an emperor in need of clothes. *Nat Neurosci* 2012;15:349–57.
- [34] Hayden EY, Teplow DB. Amyloid β -protein oligomers and Alzheimer's disease. *Alzheimers Res Ther* 2013;5:60.
- [35] Fezoui Y, Hartley DM, Harper JD, Khurana R, Walsh DM, Condron MM, et al. An improved method of preparing the amyloid β -protein for fibrillogenesis and neurotoxicity experiments. *Int J Prot Fold Dis* 2000;7:166–78.
- [36] Jan A, Hartley DM, Lashuel HA. Preparation and characterization of toxic A β aggregates for structural and functional studies in Alzheimer's disease research. *Nat Protoc* 2010;5:1186–209.
- [37] Kawashima H, Sohma Y, Nakanishi T, Kitamura H, Mukai H, Yamashita M, et al. A new class of aggregation inhibitor of amyloid- β peptide based on an O-acyl isopeptide. *Bioorg Med Chem* 2013;21:6323–7.
- [38] Walsh DM, Lomakin A, Benedek GB, Condron MM, Teplow DB. Amyloid β -protein fibrillogenesis. Detection of a protofibrillar intermediate. *J Biol Chem* 1997;272:22364–72.
- [39] Sohma Y, Hayashi Y, Kimura M, Chiyomori Y, Taniguchi A, Sasaki M, et al. The “O-acyl isopeptide method” for the synthesis of difficult sequence-containing peptides: application to the synthesis of Alzheimer's disease-related amyloid β peptide (A β) 1–42. *J Pept Sci* 2005;11:441–51.
- [40] Einstein A. Über die von der molekularkinetischen Theorie der Wärme geforderte Bewegung von in ruhenden Flüssigkeiten suspendierten Teilchen. *Ann Phys* 1905;322:549–60.
- [41] Wyttenbach T, Kemper PR, Bowers MT. Design of a new electrospray ion mobility mass spectrometer. *Int J Mass Spectrom* 2001;212:13–23.
- [42] Pringle SD, Giles K, Wildgoose JL, Williams JP, Slade SE, Thalassinos K, et al. An investigation of the mobility separation of some peptide and protein ions using a new hybrid quadrupole/travelling wave IMS/oa-ToF instrument. *Int J Mass Spectrom* 2007;261:1–12.
- [43] Wyttenbach T, Bowers MT. Gas-phase conformations: the ion mobility/ion chromatography method. *Top Curr Chem* 2003;225:207–32.
- [44] Gidden J, Ferzoco A, Baker ES, Bowers MT. Duplex formation and the onset of helicity in poly d(CG)_n oligonucleotides in a solvent-free environment. *J Am Chem Soc* 2004;126:15132–40.
- [45] Bitan G, Teplow DB. Rapid photochemical cross-linking—a new tool for studies of metastable, amyloidogenic protein assemblies. *Acc Chem Res* 2004;37:357–64.
- [46] Bitan G. Structural study of metastable amyloidogenic protein oligomers by photo-induced cross-linking of unmodified proteins. *Methods Enzymol* 2006;413:217–36.

- █ Corresponding author Department of Neurology, David Geffen School of Medicine at University of California Los Angeles, 635 Charles E. Young Drive South (Room 445), Los Angeles, CA 90095, USA.
- † We define lag phase as the period between initial sample preparation/monitoring and the beginning of continuous increases in intensity. This time is determined by establishing the point of intersection of two lines, one fitted to the initial quasi-constant intensity portion of the progress curve and the other one fitted to that portion in which persistent increases in intensity are observed. This latter curve fit also is used to establish dR_H/dt .
- † We define lag phase as the period between initial sample preparation/monitoring and the beginning of continuous increases in intensity. This time is determined by establishing the point of intersection of two lines, one fitted to the initial quasi-constant intensity portion of the progress curve and the other one fitted to that portion in which persistent increases in intensity are observed. This latter curve fit also is used to establish dR_H/dt .

Copyright © 2014 Elsevier Ltd. All rights reserved.

Note to users: Corrected proofs are Articles in Press that contain the authors' corrections. Final citation details, e.g., volume/issue number, publication year and page numbers, still need to be added and the text might change before final publication.

Although corrected proofs do not have all bibliographic details available yet, they can already be cited using the year of online publication and the DOI , as follows: author(s), article title, journal (year), DOI. Please consult the journal's reference style for the exact appearance of these elements, abbreviation of journal names and use of punctuation.

When the final article is assigned to an issue of the journal, the Article in Press version will be removed and the final version will appear in the associated published issue of the journal. The date the article was first made available online will be carried over.

Fig. S1.

QLS monitoring of i β 42-A β 42 conversion. Neutralization of (a) i β 42 and (b) Ac-i β 42 from pH 3.5 to pH 7.5. Intensity and radius plots are shown prior to and following a pH jump from 3.5 to 7.5. Red arrows indicate the time at which neutralization was performed.

**Fig. S2.**

QLS monitoring of A β assembly kinetics. Plot of hydrodynamic radius (R_H) versus elapsed time (h) for A β 42, i β 42, and Ac-i β 42 at pH 7.5. Lines were produced using the linear regression curve fit capability of KaleidaGraph v4.1 (Synergy Software, Reading, PA).

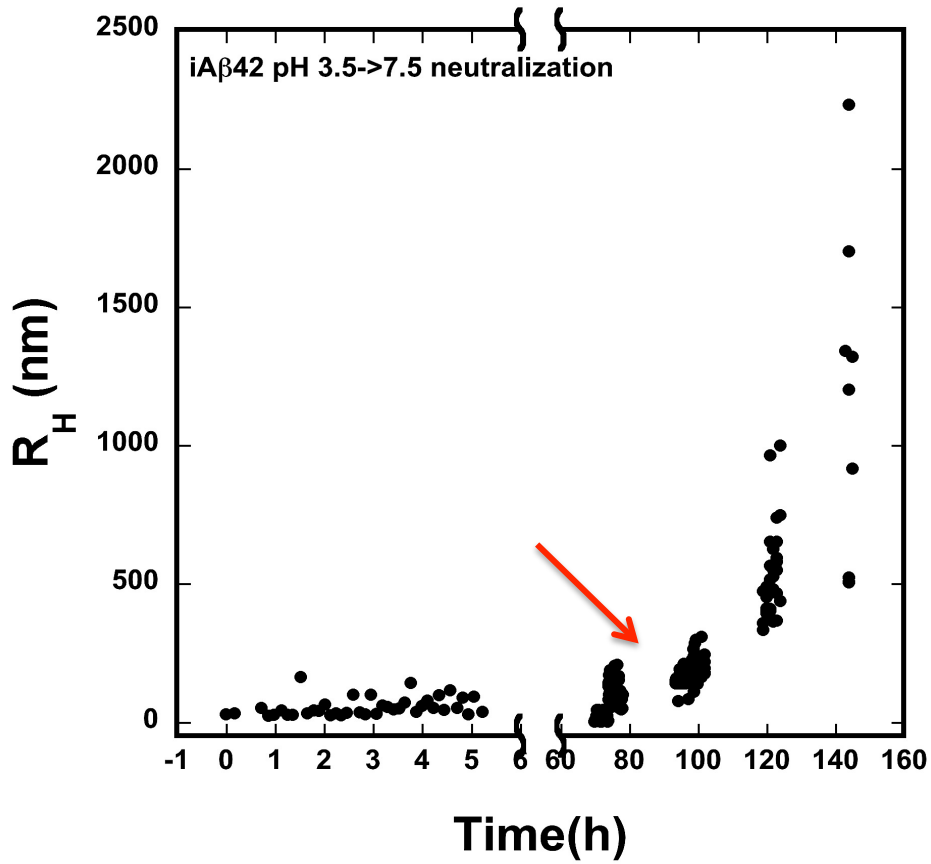
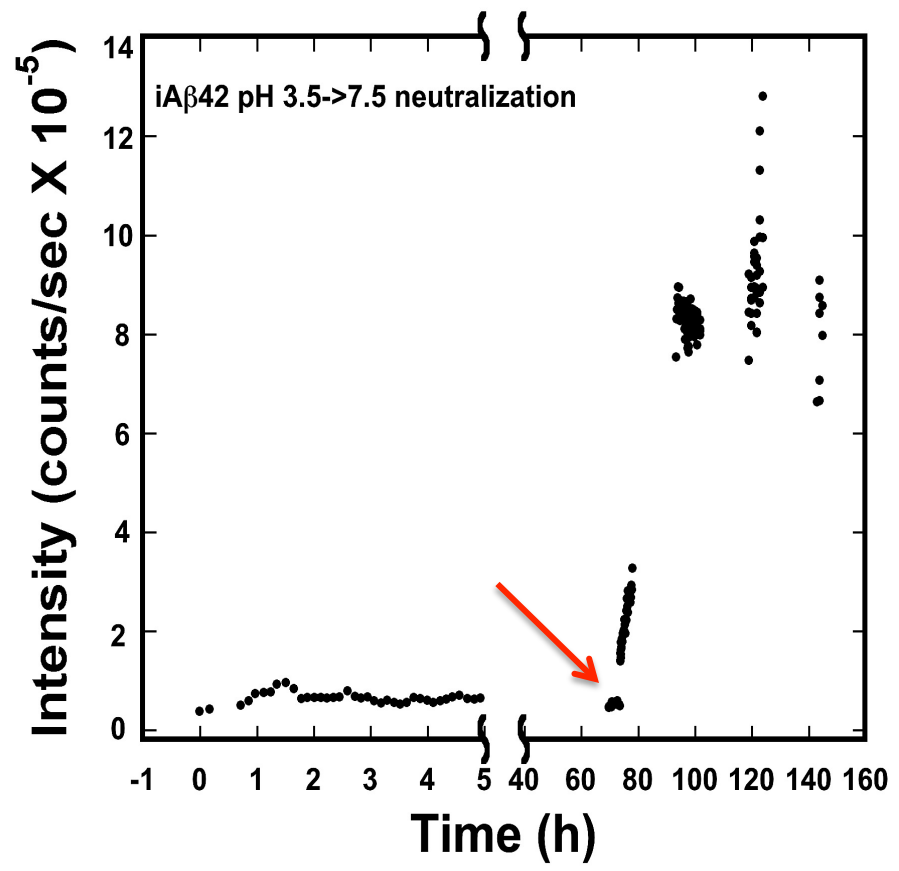
[Help with PPTX files](#)[Options ▾](#)**Fig. S3.**

Mass spectra of i β 42 and Ac-i β 42. Mass spectra of i β 42 in 25 mM ammonium acetate, pH 7.4, at (a) 20 min and (b) 2 h after dissolution. Mass spectra of Ac-i β 42 in (c) 10 mM and (d) in 0.1 mM ammonium acetate buffer, pH 7.4, at a final peptide concentration of 30 μ M.

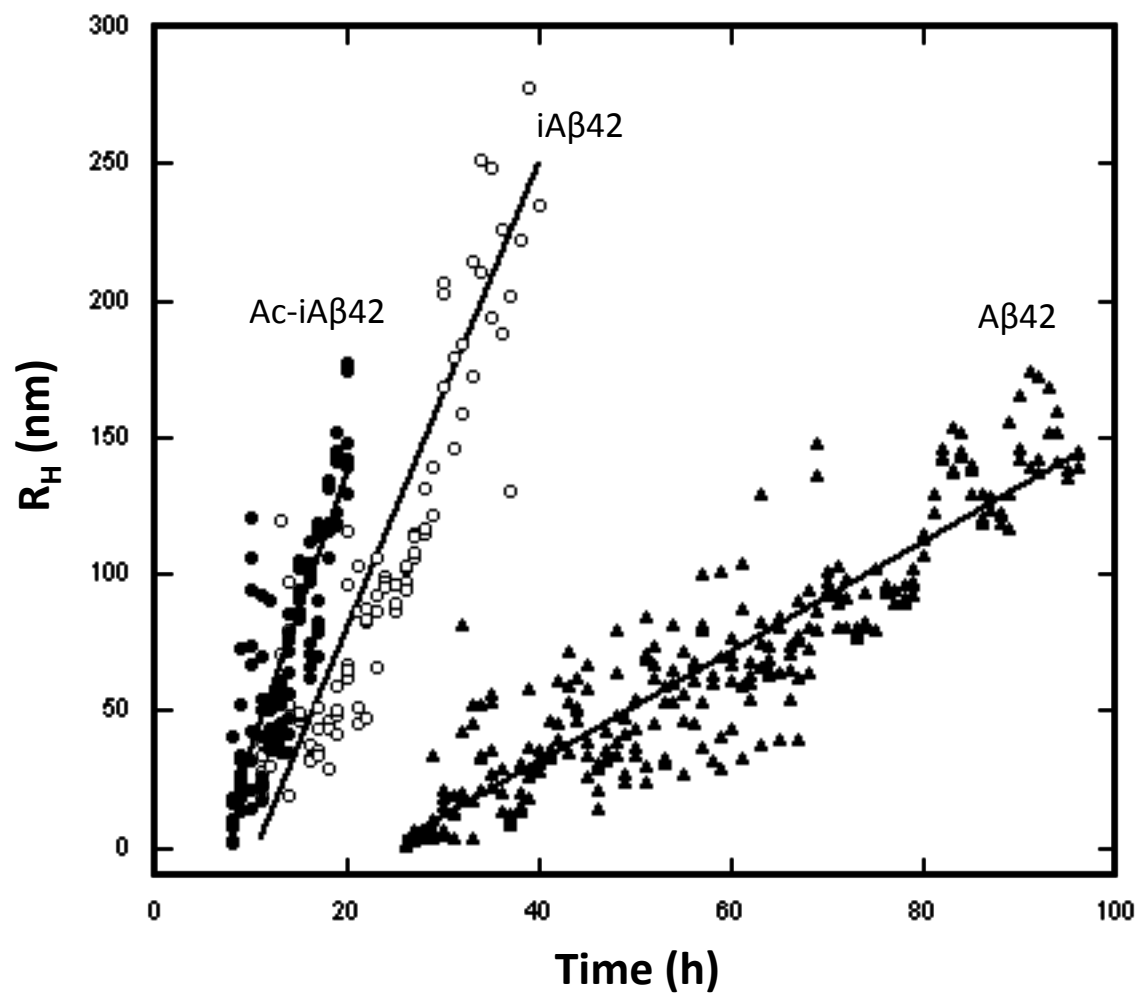
[Help with PPTX files](#)[Options ▾](#)**Fig. S4.**

IMS-MS analysis of $z/n = 5/2$ charge states. Comparison of (a) A β 42, (b) i β 42, and (c) Ac-i β 42 at injection voltage of 50 V. The ATDs are plotted as a function of σ/n to normalize differing experimental conditions.

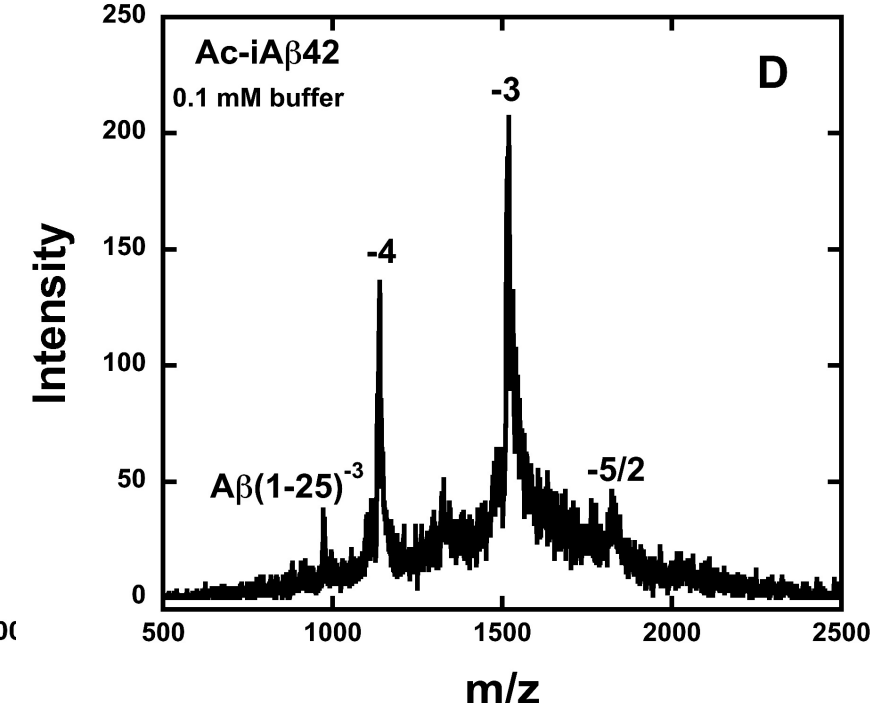
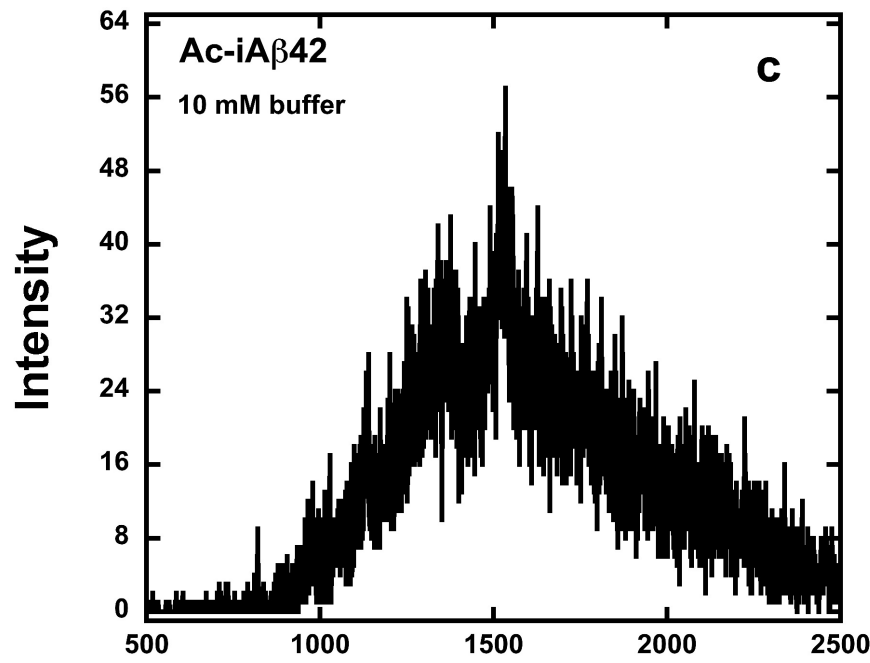
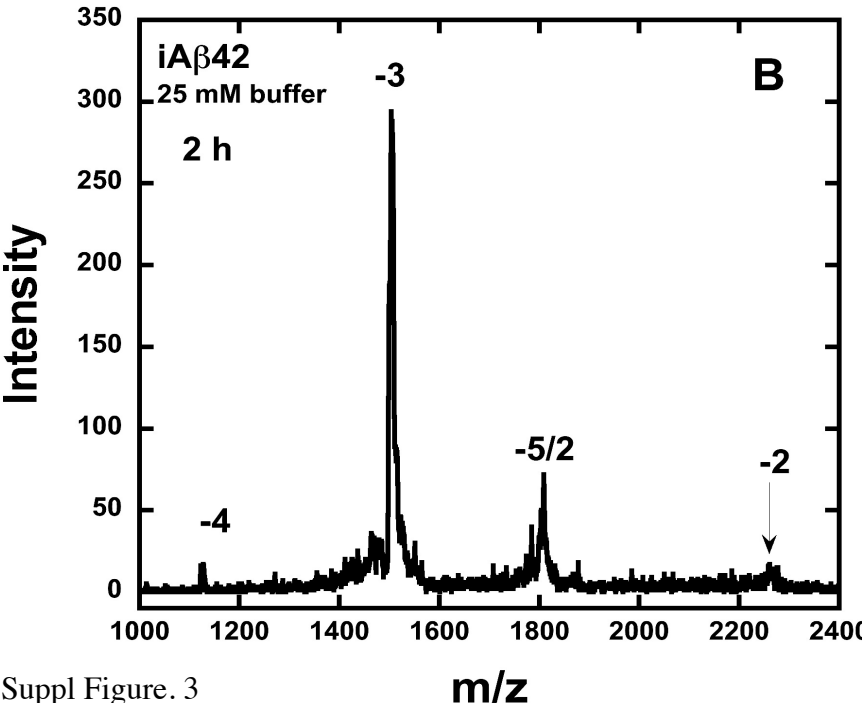
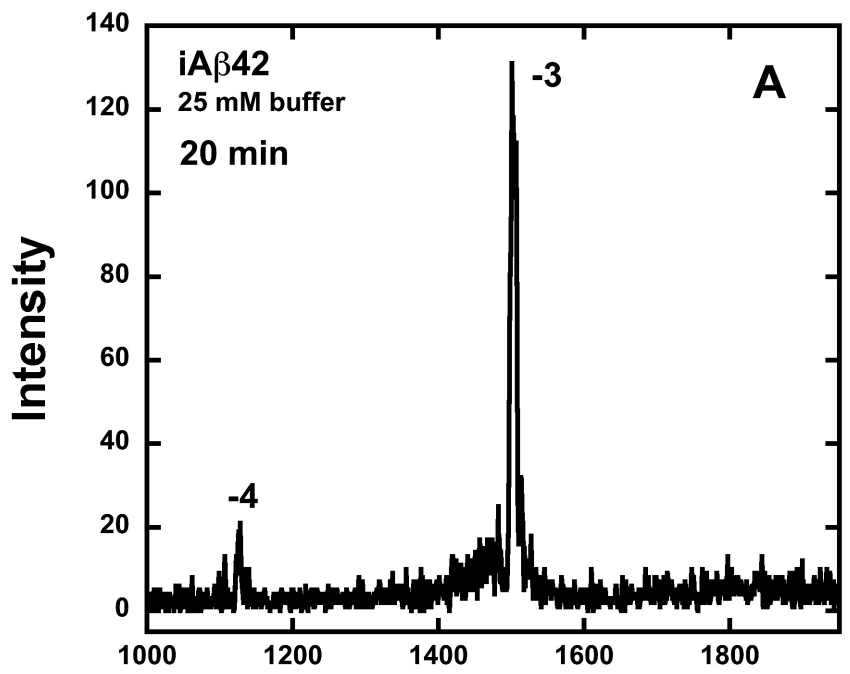
A



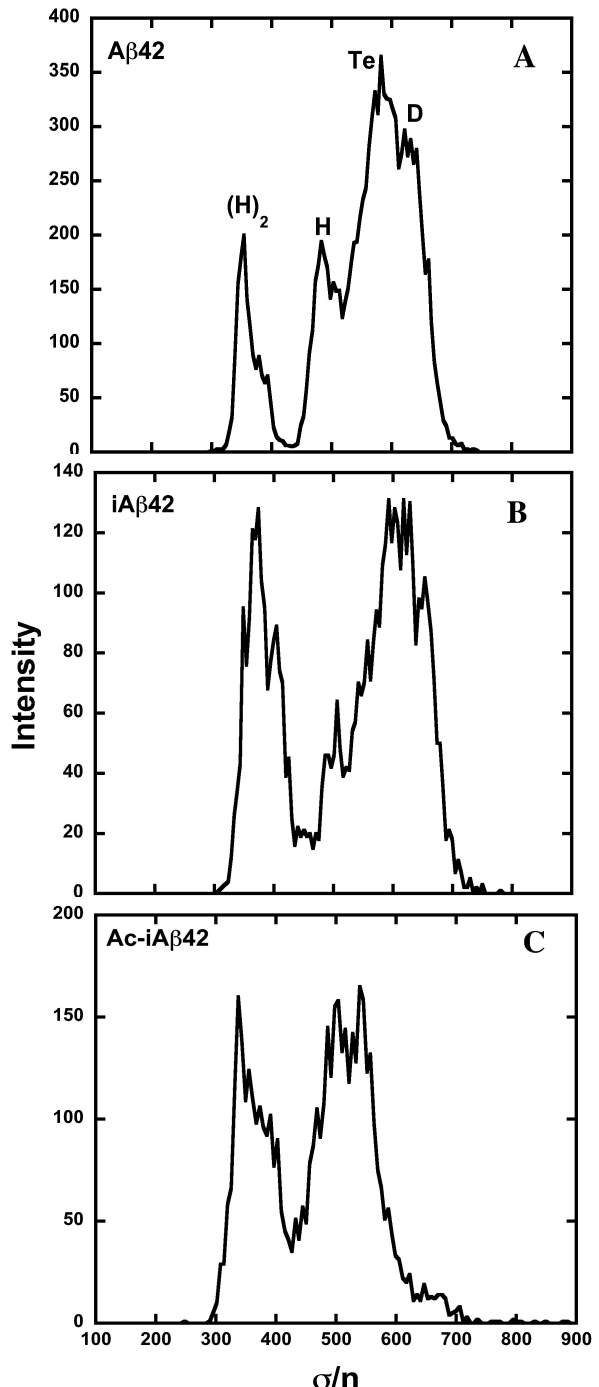
Suppl Figure. 1



Suppl Figure. 2



Suppl Figure. 3



Suppl Figure. 4